Three-dimensional multispecies hybrid simulation of Titan's highly variable plasma environment

S. Simon, A. Boesswetter, T. Bagdonat, U. Motschmann, J. Schuele

Ann. Geophys., 25, 117–144, 2007
www.ann-geophys.net/25/117/2007/

Annales Geophysicae

Three-dimensional multispecies hybrid simulation of Titan's highly variable plasma environment

S. Simon[1], **A. Boesswetter**[1], **T. Bagdonat**[1], **U. Motschmann**[1,2], **and J. Schuele**[3]

[1]Institute for Theoretical Physics, TU Braunschweig, Germany
[2]Institute for Planetary Research, DLR, Berlin, Germany
[3]Institute for Scientific Computing, TU Braunschweig, Germany

Received: 18 July 2006 – Revised: 4 December 2006 – Accepted: 6 December 2006 – Published: 1 February 2007

Abstract. The interaction between Titan's ionosphere and the Saturnian magnetospheric plasma flow has been studied by means of a three-dimensional (3-D) hybrid simulation code. In the hybrid model, the electrons form a mass-less, charge-neutralizing fluid, whereas a completely kinetic approach is retained to describe ion dynamics. The model includes up to three ionospheric and two magnetospheric ion species. The interaction gives rise to a pronounced magnetic draping pattern and an ionospheric tail that is highly asymmetric with respect to the direction of the convective electric field. Due to the dependence of the ion gyroradii on the ion mass, ions of different masses become spatially dispersed in the tail region. Therefore, Titan's ionospheric tail may be considered a mass-spectrometer, allowing to distinguish between ion species of different masses. The kinetic nature of this effect is emphasized by comparing the simulation with the results obtained from a simple analytical test-particle model of the pick-up process. Besides, the results clearly illustrate the necessity of taking into account the multi-species nature of the magnetospheric plasma flow in the vicinity of Titan. On the one hand, heavy magnetospheric particles, such as atomic Nitrogen or Oxygen, experience only a slight modification of their flow pattern. On the other hand, light ionospheric ions, e.g. atomic Hydrogen, are clearly deflected around the obstacle, yielding a widening of the magnetic draping pattern perpendicular to the flow direction. The simulation results clearly indicate that the nature of this interaction process, especially the formation of sharply pronounced plasma boundaries in the vicinity of Titan, is extremely sensitive to both the temperature of the magnetospheric ions and the orientation of Titan's dayside ionosphere with respect to the corotating magnetospheric plasma flow.

Correspondence to: S. Simon
(sven.simon@tu-bs.de)

Keywords. Magnetospheric physics (Magnetosphere interactions with satellites and rings; Magnetosphere-ionosphere interactions) – Space plasma physics (Kinetic and MHD theory; Numerical simulation studies)

1 Introduction

In the year 2004, ESA and NASA scientists celebrated the arrival of the Cassini spacecraft in the Saturnian system, marking the beginning of an extensive exploration of the giant planet and its complex system of rings and satellites. One of the major objectives of the mission is the exploration of Titan, Saturn's largest moon. The T_A flyby on 26 October 2004 was the first visit of a spacecraft since the pass of Voyager 1 more than 20 years ago. One of the most interesting aspects of Titan is its extremely complex and variable interaction with the surrounding plasma.

As both Voyager 1 and Cassini measurements have shown that Titan does not possess a noticeable intrinsic magnetic field (Ness et al., 1982; Backes et al., 2005), Titan's ionosphere interacts directly with the impinging plasma flow. For the case of Titan being located inside Saturn's magnetosphere, the obstacle faces the hot and slow magnetospheric plasma, providing a variety of different interaction scenarios. On the one hand, depending on Titan's orbital position, the dayside ionosphere is not necessarily located at the ramside of the satellite. On the other hand, both Voyager 1 and Cassini measurements indicate that the Mach numbers of the impinging magnetospheric plasma flow are also a function of Titan's orbital position (Wolf and Neubauer, 1982; Ledvina et al., 2004; Ma et al., 2006). When Saturn's magnetosphere is compressed due to high solar wind dynamic pressure, Titan's plasma environment is likely to undergo the most remarkable transition, as the satellite is capable of

Published by Copernicus GmbH on behalf of the European Geosciences Union.

leaving Saturn's magnetosphere in the subsolar region of its orbit and interact directly with the solar wind. Such extreme solar wind conditions have been observed during the visit of Pioneer 11 in the Saturnian system (Schardt et al., 1984). The strong analogy between the Titan scenario and the interaction between the unmagetized planets Venus and Mars with their plasma environment has been emphasized in several comparative studies (Kivelson and Russell, 1983; Verigin et al., 1984; Luhmann et al., 1991).

During the last decade, Titan's plasma interaction has been the subject of numerous numerical simulation studies. Magnetohydrodynamic and multi-fluid approaches, such as the models developed by Keller et al. (1994), Keller and Cravens (1994), Cravens et al. (1998), Ledvina and Cravens (1998), Kabin et al. (1999, 2000), Kopp and Ip (2001), Nagy et al. (2001) and Ma et al. (2004), are able to provide a global picture of Titan's plasma interaction and have, for instance, shown to be able to reproduce the magnetic field signature observed during the Voyager 1 flyby. However, due to the characteristic length scales of the interaction region being comparable to the mean ion gyroradii in the ambient magnetospheric plasma flow, the fluid approximation is not strictly applicable to the case of Titan. Specifically, the MHD models are unable to reproduce the highly asymmetric structure of Titan's ionospheric tail, as it has e.g. been detected during the first Cassini flybys (Wahlund et al., 2005). However, these features of Titan's plasma interaction can be explained in the framework of the hybrid model, retaining the particle character of the ionospheric ions. The first who applied the hybrid model to the case of Titan were Brecht et al. (2000). The results of this simulation study indicate that the magnetic pile-up region at Titan's ramside exhibits a definite preference to expand into the hemisphere where the convective electric field is directed away from Titan. Brecht et al. (2000) were also the first who studied the influence of different ionospheric pick-up masses in the framework of the hybrid model. However, the model used by Brecht et al. (2000) did not consider the extremely high temperature of the impinging magnetospheric plasma flow, i.e. the temperatures of both electrons and ions were set to zero. Even though the hybrid model presented by Kallio et al. (2004) was the first kinetic approach to retain the finite ion temperature, the finite electron temperature has been neglected. The same simplifying assumption has been used by Sillanpää et al. (2006). The first hybrid model that considered both the electron and ion temperature and was even able to distinguish between magnetospheric and ionospheric electrons has been presented by Simon et al. (2006c,b). Since this code allows to conduct simulations on an arbritrary curvilinear grid (Bagdonat and Motschmann, 2001, 2002a,b; Bagdonat, 2004; Bößwetter et al., 2004), the simulations could be carried out on a grid with spherical symmetry that can be adapted to the geometry of the obstacle. This simulation approach allowed a detailed analysis of Titan's plasma interaction, focussing on the dependence of the magnetic field topology on the satellite's orbital position and on the analysis of the highly asymmetric tail structure. The simulations carried out by Simon et al. (2006c,b) have also shown hat the mechanism giving rise to both the asymmetric tail structure and to a so-called Ion Composition Boundary when the obstacle leaves the magnetosphere can be understood in strong analogy to the Martian interaction with the solar wind, as discussed by Bößwetter et al. (2004).

However, in earlier hybrid simulation studies, Titan's plasma environment has been analyzed in terms of a two-species hybrid model. The results allowed to obtain a general picture of how the major features of the satellite's plasma environment change as a function of orbital position. Nevertheless, the real Titan situation is significantly more complex.

On the one hand, numerous ionospheric models, especially those designed by Keller et al. (1992, 1994, 1998), Keller and Cravens (1994), and Cravens et al. (2006) clearly illustrate that Titan's ionosphere exhibits a complex ion chemistry and that interaction processes between different species make up a major feature of this region. These aspects can be taken into account by magnetohydrodynamic models of Titan's plasma environment (cf. Ma et al., 2004, 2006; Backes et al., 2005; Backes, 2005). However, covering these features of Titan's plasma environment in the framework of hybrid simulations is presently difficult. Even a parallel computer would be incapable of storing the data of a sufficiently high number of particles. Of course, one could design a simulation scenario that allows an extremely high spatial resolution in the immediate vicinity of the obstacle. However, it is presently impossible to create a simulation scenario that allows more than 90 grid nodes in each spatial direction. Therefore, in such a scenario Titan itself would fill almost the entire simulation domain, i.e. the outer boundaries of the simulation box would be located quite close to the interaction region and would possibly affect the plasma flow in the vicinity of Titan. For this reason, enhancing the spatial resolution of the ionosphere region by reducing the total size of the simulation box is definitely not an option. Using a curvilinear simulation grid, as also suggested by Bagdonat (2004) and Bößwetter et al. (2004), is a step in the direction of achieving a sufficient resolution in Titan's ionosphere region, but even by means of this grid, it is impossible to gain access to spatial scales below $0.1\,R_T$. Besides, when increasing the curvature of the grid, it becomes more and more likely that numerical stability is compromised. For this reason, a hybrid simulation including a detailed multispecies model of Titan's ionosphere is beyond the scope of any existing simulation code. Nevertheless, the first question that such a multi-species ionosphere model should adress is how the presence of severel species of different mass would affect the global structure of the ionospheric tail. For this reason, the first stage of expansion for the model used by Simon et al. (2006c) is the incorporation of a simple production profile for several different ionospheric species.

On the other hand, according to Voyager 1 measurements (Neubauer et al., 1984), the upstream plasma flow in the vicinity of Titan consists of two major species, Hydrogen and Nitrogen (or Oxygen which possesses a comparable mass). For the simulations that have been presented by Simon et al. (2006c,b), these upstream plasma conditions have been approximated by using a singe ion species with an average particle mass and number density. The simulation results have shown that for the case of Titan being located inside Saturn's magnetosphere, the ambient plasma density and velocity are not significantly affected by the presence of the obstacle. Of course, a region of reduced plasma density and velocity manifests downstream of Titan, but nevertheless, the effect on the upstream flow is definitely not as significant as in the case of Titan being exposed to a supersonic plasma flow. As the two species that make up the upstream flow inside Saturn's magnetosphere have siginificantly different masses, it must be expected that the plasma densities and velocities of Nitrogen and Hydrogen are modified on different scales. In general, the smaller is the ion mass of an upstream species, the more significant should be the acceleration of the respective ions by the Lorentz force. For this reason, splitting up the upstream plasma flow in two different species is a necessary extension of the models presented in former papers.

The extension of the hybrid code to the case of multi-species conditions has been realized in two different steps:

– In the first step, two additional ionospheric species have been incorporated into the model. In agreement with Modolo (2004), Titan's ionosphere is assumed to be consisting of molecular Nitrogen (N_2^+), Methane (CH_4^+) and molecular Hydrogen (H_2^+). The upstream plasma flow, on the other hand, is still assumed to be consisting of a single species of mass m=9.6 amu and density n=0.3×10^6 m^{-3} (see also Kallio et al., 2004; Sillanpää et al., 2006). In the following, this species will be referred to as the (N^+/H^+) mixed plasma. Hence, the model will include one species (N_2^+) which is significantly heavier than the upstream plasma species, another species (CH_4^+) whose mass is comparable to the ion mass in the upstream plasma flow, and finally a third species whose mass is around a factor 5 smaller than the ion mass in the upstream flow. Such an extension of the model should at least allow to identify major features of the ionospheric tail structure as a function of the relative ion mass as well as changes in the overall magnetic field topology arising from the multi-species description of the ionosphere. At the present stage, a high resolutive study of the ionosphere region must be left to MHD models. However, in contrast to fluid approaches, the model will provide the first self-consistent description of Titan's plasma environment that considers the influence of finite gryoradius effects under multi-species conditions.

– In the second step, the multi-species ionosphere has been retained. In addition, the upstream plasma flow will be splitted up in the two species that have been detected during the Voyager 1 flyby. Hence, the simulation scenario will include five different ion species. Due to the high number of particles, this kind of simulation requires a huge amount of storage capacity. These simulations are expected to allow a detailed analysis of Titan's effect on the upstream plasma flow.

After discussing the major features of the multi-species hybrid code in the next section, the results of the simulations will be presented. A simplifying analytical model of the pick-up process at Titan will allow to validate the simulation approach. In addition, the applicability of the different simulation approaches to the plasma environment of Titan will be analyzed in an extensive comparative discussion.

2 The hybrid model

2.1 Basic assumptions

The simulations are carried out by using a three-dimensional hybrid code that can operate on an arbitrary curvilinear grid (Bagdonat and Motschmann, 2001, 2002a,b; Bagdonat, 2004). The present version of the code has already been successfully applied to the solar wind interaction with magnetized asteroids (Simon et al., 2006a) as well as to the plasma environments of Mars (Bößwetter et al., 2004) and Titan (Simon et al., 2006c,b). Since an extensive discussion of the major features of the simulation code is given in earlier papers, only a short overview of the most important aspects will be presented in the following paragraphs.

In the hybrid model, the electrons are treated as a massless, charge-neutralizing fluid, whereas all ion species occuring in the simulation are represented by macroparticles. The basic equations of this model can be written as follows:

– Equations of motion for individual ions:

$$\frac{\mathrm{d}\boldsymbol{x}_s}{\mathrm{d}t} = \boldsymbol{v}_s \quad \text{and} \quad \frac{\mathrm{d}\boldsymbol{v}_s}{\mathrm{d}t} = \frac{q_s}{m_s}\left\{\boldsymbol{E} + \boldsymbol{v}_s \times \boldsymbol{B}\right\}, \qquad (1)$$

where $\boldsymbol{x}_s$ and $\boldsymbol{v}_s$ denote the position and the velocity of an ion of species s, respectively. The vectors $\boldsymbol{E}$ and $\boldsymbol{B}$ are the electromagnetic fields.

– Electric field equation: Simon et al. (2006c) have introduced the basic concept of a hybrid model for Titan that includes two different electron fluids, one for the magnetospheric and one for the ionospheric electrons. This discussion can easily be generalized to the case of a hybrid code that takes into account an arbitrary number of N ion species. In consequence, N different electron species (with different temperatures) should be incorporated into the model. In the following, the electric field equation for such a scenario will be briefly discussed.

It is assumed that the simulation contains N different ion species whose electron populations possess, in general, significantly different properties. The subscript j (j=1, ..., N) is introduced to distinguish between different ion species and the corresponding electron populations. However, at this point, it is not relevant whether the ions are of magnetospheric or of ionospheric origin. The dynamics of each electron population are described by the momentum equation

$$0 = -en_{e,j}\left(\boldsymbol{E} + \boldsymbol{u}_{e,j} \times \boldsymbol{B}\right) - \nabla P_{e,j} \quad ; \tag{2}$$

j=1, ..., N. The quantities $n_{e,j}$, $\boldsymbol{u}_{e,j}$ and $P_{e,j}$ denote the mean density, velocity and pressure of electron species j, respectively. In order to obtain a single equation for the electric field, the N momentum equations (2) are added, yielding

$$0 = -e\boldsymbol{E}\sum_{j=1}^{N} n_{e,j} - e\left(\sum_{j=1}^{N} n_{e,j}\boldsymbol{u}_{e,j}\right) \times \boldsymbol{B} - \\ -\sum_{j=1}^{N} \nabla P_{e,j} \quad . \tag{3}$$

In analogy to the hybrid model with two electron populations, a total electron density n_e is introduced by means of

$$n_e \equiv \sum_{j=1}^{N} n_{e,j} \quad . \tag{4}$$

In exactly the same manner, a mean electron velocity can be defined by means of

$$\boldsymbol{u}_e \equiv \frac{1}{n_e}\sum_{j=1}^{N} n_{e,j}\boldsymbol{u}_{e,j} \quad . \tag{5}$$

Hence, the electric field reads

$$\boldsymbol{E} = -\boldsymbol{u}_e \times \boldsymbol{B} - \frac{\sum_{j=1}^{N} \nabla P_{e,j}}{en_e} \quad . \tag{6}$$

Introducing the total electron current density $\boldsymbol{j}_e$=$-en_e\boldsymbol{u}_e$ and the charge density ρ_c=en_e=en_i (n_i: total ion density) yields

$$\boldsymbol{E} = -\boldsymbol{u}_i \times \boldsymbol{B} + \frac{(\nabla \times \boldsymbol{B}) \times \boldsymbol{B}}{\mu_0 \rho_c} - \frac{\sum_{j=1}^{N} \nabla P_{e,j}}{\rho_c} \tag{7}$$

for the electric field. In this expression, $\boldsymbol{u}_i$ denotes the mean ion velocity at the respective position. However, it is important to notice that the simulation model is able to distinguish between different ion densities *and* velocities, whereas it takes into account only a single electron velocity $\boldsymbol{u}_e$. The distinguishment between the electron populations corresponding to different ion species is realized only by means of the electron pressure terms. For the simulations discussed in this paper, the electrons are assumed to be adiabatic, i.e.

$$p_e \propto \beta_{e,j}\left(n_{e,j}\right)^{\kappa} \quad ; \quad j = 1, \ldots, N \quad , \tag{8}$$

where $\beta_{e,j}$ are the plasma betas of the different electron populations, allowing to introduce an independent temperature for each of them. A value of κ =2 has been chosen for the adiabatic exponent (Bößwetter et al., 2004; Simon et al., 2006a,c,b). By including this set of N coupling expressions, a closed set of equations is obtained.

– Magnetic field equation: by using Faraday's law, an expression describing the time evolution of the magnetic field is obtained:

$$\frac{\partial \boldsymbol{B}}{\partial t} = \nabla \times (\boldsymbol{u}_i \times \boldsymbol{B}) - \nabla \times \left[\frac{(\nabla \times \boldsymbol{B}) \times \boldsymbol{B}}{\mu_0 e n_e}\right] . \tag{9}$$

Because of the adiabatic description of the electrons, the electron pressure terms do not occur in this equation.

2.2 Simulation geometry and parameters

The simulation box possesses an extension of $\pm 7.5\,R_T$ (R_T=2575 km) in each spatial direction; the center of Titan coincides with the origin of the coordinate system. The simulations are carried out on a curvilinear simulation grid (a so-called *Fisheye Grid*) which can be adapted to the spherical geometry of the obstacle. It also allows a high spatial resolution in the immediate vicinity of the planet. This grid is obtained from an equidistant Cartesian grid by means of a non-linear coordinate transformation (cf. Bagdonat, 2004; Bößwetter et al., 2004). In each spatial direction, the simulation grid consists of 90 grid nodes. In correspondence to our earlier simulations, the upstream magnetospheric plasma parameters have been chosen in agreement with Voyager 1 data, as presented by Neubauer et al. (1984): The undisturbed magnetic field strength is B_0=5 nT, the field vector is directed perpendicular to Titan's orbital plane. A value of u_0=120 km/s has been chosen for the upstream plasma velocity. In the simulations using a single-species representation for the magnetospheric plasma flow, the upstream ion species is characterized by a mass of m=9.6 amu and a number density of n=0.3×10^6 m^{-3}. These parameters may be considered average values obtained from the Voyager 1 data. On the other hand, in the simulations applying a multi-species model to the magnetospheric flow, two different ion species, Nitrogen (N^+) and Hydrogen (H^+) , have been incorporated into the simulation model. It should be noticed that, even though this does not take noticeable influence on the simulation results, recent Cassini measurements indicate

Oxygen (O^+) to be the predominant species in the magnetosphere.

Their upstream densities are given by $n(N^+)=0.2\times10^6$ m^{-3} and $n(H^+)=0.5\,n(N^+)$; the corresponding temperatures are $k_BT(N^+)=2900$ eV and $k_BT(H^+)=210$ eV. In all simulation runs, the temperature of the charge-neutralizing magnetospheric electron population has been set to a value of $k_BT_e=200$ eV. The parameters given above yield the following set of Mach numbers for the impinging magnetospheric plasma: $M_A=1.9$ (alfvenic), $M_S=0.57$ (sonic) and $M_{MS}=0.55$ (magnetosonic). Due to the subsonic nature of the magnetospheric flow, no bow shock will form in front of Titan. A value of $k_BT_e=0.1$ eV has been chosen for the ionospheric electron temperatures, which is in good agreement with the models discussed by Roboz and Nagy (1994) as well as Nagy and Cravens (1998).

The inner boundary of the simulation obstacle is located at an altitude of $R_0=1100$ km above the surface of Titan. This boundary is assumed to be absorptive, i.e. any particle hitting the sphere is removed from the simulation. In contrast to this, no boundary conditions are imposed on the electromagnetic fields (cf. Bößwetter et al., 2004; Simon et al., 2006c).

The ionosphere is assumed to be a spherical shell with the inner radius R_0 and with an outer radius of 3 R_T. The obstacle's dayside ionosphere is represented by a Chapman layer, i.e. photoionization is assumed to be the dominant source of newly generated ionospheric ions. Thus, the production profile $q(r, \chi)$ depends on both the altitude r above the surface and the solar zenith angle χ. The nightside production profile is assumed to be independent of the solar zenith angle and is given by $q=q(r, \chi=87°)$. For each ionospheric species, the total production rate is set to a value of $Q=1.3\times10^{25}$ s^{-1}. An extensive description of our ionosphere model has been given by Bößwetter et al. (2004) and in the companion Titan papers. In order to achieve a stationary state, the total duration of the simulations corresponds to a time in which the undisturbed magnetospheric plasma passes through the entire simulation domain 30−40 times. Each simulation scenario contains more than 12 million macroparticles. In the following section, the subscripts m and i are used to distinguish between particles of magnetospheric and ionospheric origin.

It should be noted that in the following sections, the term *two-species hybrid model* refers to earlier simulation attempts assuming the magnetospheric plasma to consist of a single species, while another species is used to represent the ionosphere. The term *multi-species hybrid model* refers to any scenario taking into account more than two ion species.

3 Ion pick-up at Titan

In order to understand the simulation results presented in the following sections, it is useful to discuss the ion pick-up process at Titan from a qualitative point of view at first. Specifically, the analysis refers to a single ionospheric particle of mass m and charge e which is inserted into the ambient magnetospheric plasma flow. The particle's equation of motion reads

$$\ddot{\boldsymbol{x}} = \dot{\boldsymbol{v}} = \frac{e}{m}\left(\boldsymbol{E} + \boldsymbol{v}\times\boldsymbol{B}\right) , \tag{10}$$

where $\boldsymbol{x}$ and $\boldsymbol{v}$ denote its position and velocity, respectively.

The discussion refers to the case of Titan being located inside Saturn's magnetosphere at 18:00 Saturnian local time, i.e. the dayside of the obstacle faces the corotating magnetospheric plasma flow. The geometry of this scenario is displayed in Fig. 1. The undisturbed magnetospheric plasma flow is directed parallel to the (+x)-axis, whereas the homogeneous background magnetic field is pointing in (-z)-direction. Therefore, the convective electric field $\boldsymbol{E}_c$ is oriented antiparallel to the y-axis.

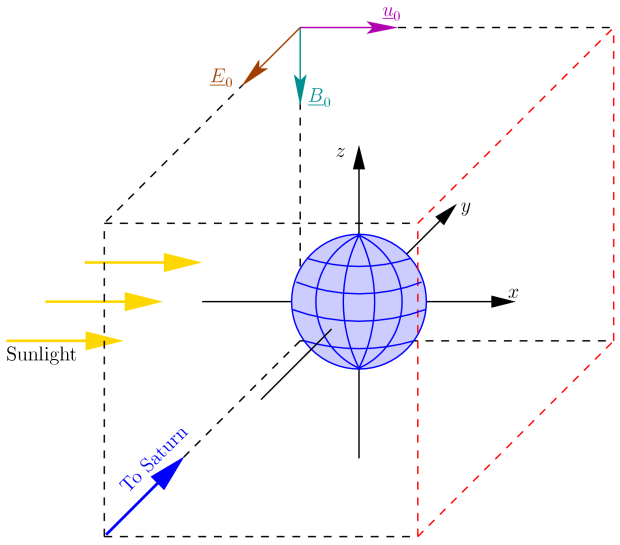

Fig. 1. Simulation geometry. The simulation box possesses a spatial extension of $\pm7.5\,R_T$ in each spatial direction; the center of Titan coincides with the origin of the Cartesian coordinate system. In all simulations presented in this work, the (+x)-axis is directed from the sun to Titan, referring to the situation at the equinoxes of Saturn's orbital period. In the 18:00 local time scenario, which is displayed in the figure, the upstream magnetospheric plasma flow is directed parallel to the (+x)-direction, whereas the homogeneous background magnetic field is oriented antiparallel to the z-axis. Thus, the convective electric field vector is pointing in the (y<0)-direction, away from Saturn. The face of the simulation box that is located in Titan's wake region is denoted by red lines. The second situation that has been investigated is the case of Titan's nightside being exposed to the upstream plasma flow at 06:00 local time. The simulation geometry is the same as in the 18:00 case, except for the undisturbed magnetospheric plasma flow being directed antiparallel to the (+x)-axis. Thus, the convective electric field points in (+y)-direction, but – in analogy to the 18:00 local time scenario – is again directed away from Saturn.

Assuming that the electric field in the tail region is mainly governed by the convective term $\boldsymbol{E}_c = -\boldsymbol{u}_m \times \boldsymbol{B}$, as stated by Simon et al. (2006c), yields

$$\dot{\boldsymbol{v}} = \frac{e}{m}\,(-\boldsymbol{u}_m + \boldsymbol{v}) \times \boldsymbol{B} \quad . \tag{11}$$

In this expression, $\boldsymbol{u}_m$ denotes the mean magnetospheric plasma velocity. In the following, the discussion focusses on the situation in Titan's equatorial plane where, according to earlier simulation results, the magnetospheric plasma velocity is not significantly distorted by the presence of the obstacle. Therefore, without losing generality, $\boldsymbol{u}_m$ is assumed to be directed parallel to the x-axis,

$$\boldsymbol{u}_m = \begin{pmatrix} u_m \\ 0 \\ 0 \end{pmatrix} \quad . \tag{12}$$

For simplicity, u_m is assumed to be spatially constant. Even in the case of highly draped field lines, the magnetic field is oriented almost perpendicular to the equatorial plane, i.e.

$$\boldsymbol{B} = \begin{pmatrix} 0 \\ 0 \\ B \end{pmatrix} \quad , \tag{13}$$

where B is negative and, for simplicity, is assumed to be spatially constant. Now, Eq. (11) is transformed into the rest frame of the plasma by means of the Galilei transformation:

$$\boldsymbol{\mathcal{V}} = \boldsymbol{v} - \boldsymbol{u}_m \quad . \tag{14}$$

The transformed equation of motion is

$$\dot{\boldsymbol{\mathcal{V}}} = \frac{e}{m}\boldsymbol{\mathcal{V}} \times \boldsymbol{B} \quad \text{or equivalently} \quad \dot{\boldsymbol{\mathcal{V}}} = \underline{\underline{M}} \cdot \boldsymbol{\mathcal{V}} \tag{15}$$

with the 3×3 matrix

$$\underline{\underline{M}} = \begin{pmatrix} 0 & \Omega & 0 \\ -\Omega & 0 & 0 \\ 0 & 0 & 0 \end{pmatrix} \quad . \tag{16}$$

The ion gyrofrequency is given by

$$\Omega = \frac{eB}{m} \quad . \tag{17}$$

The solution of Eq. (15) is obtained by diagonalizing the matrix $\underline{\underline{M}}$ and can be written as

$$\boldsymbol{\mathcal{V}} = \xi_1 \begin{pmatrix} 0 \\ 0 \\ 1 \end{pmatrix} + \xi_2 \exp(i\Omega t) \begin{pmatrix} 1 \\ i \\ 0 \end{pmatrix} + \\ + \xi_3 \exp(-i\Omega t) \begin{pmatrix} 1 \\ -i \\ 0 \end{pmatrix} \quad , \tag{18}$$

where ξ_1, ξ_2 and ξ_3 are integration constants. Transforming $\boldsymbol{\mathcal{V}}$ in the rest frame of Titan by means of Eq. (14) and assuming that the ionospheric particle's initial velocity at $t=0$ is negligible, i.e. $\boldsymbol{v}(t=0)=0$, yields

$$v_x(t) = u_m\,(1 - \cos\Omega t) \quad ; \tag{19}$$

$$v_y(t) = u_m \sin\Omega t \quad ; \tag{20}$$

$$v_z(t) = 0 \quad . \tag{21}$$

The cosinus and sinus terms in Eqs. (19) and (20) represent the particle's gyration in the plasma rest frame. Due to the constant term in Eq. (19), a uniform motion in x-direction is imposed on this circular trajectory. Assuming that the particle is inserted into the ambient plasma flow at point $\boldsymbol{x}(t=0)=(0,0,0)$ leads to the following expressions for the particle trajectory:

$$x(t) = \frac{u_m}{\Omega}\,(\Omega t - \sin\Omega t) \quad ; \tag{22}$$

$$y(t) = \frac{u_m}{\Omega}\,(1 - \cos\Omega t) \quad ; \tag{23}$$

$$z(t) = 0 \quad . \tag{24}$$

Hence, the pick-up ion moves in a plane perpendicular to the magnetic field, i.e. it remains confined to Titan's equatorial plane in the simplified case discussed here. It is important to notice that, due to $B<0$, the ion gyrofrequency Ω is negative. By introducing

$$|\Omega| = -\frac{eB}{m} \tag{25}$$

and the ion gyroradius

$$R_g = \frac{u_m}{|\Omega|} \quad , \tag{26}$$

the particle trajectory takes the form

$$x(t) = R_g\,(|\Omega|\,t - \sin|\Omega|\,t) \quad ; \tag{27}$$

$$y(t) = R_g\,(\cos|\Omega|\,t - 1) \quad ; \tag{28}$$

$$z(t) = 0 \quad . \tag{29}$$

According to Eqs. (27–29), the ionospheric ion performs a cycloidal motion in the plane perpendicular to the magnetic field, as displayed in Fig. 2. The height h of one arc of the cycloid is given by

$$h = \left| y\left(t = \frac{\pi}{|\Omega|}\right)\right| = 2R_g = 2\frac{u_m m}{e|B|} \quad , \tag{30}$$

whereas its width w can be written as

$$w = x\left(t = \frac{2\pi}{|\Omega|}\right) - x(t=0) \\ = 2\pi R_g = 2\pi\frac{u_m m}{e|B|} = \pi h \quad . \tag{31}$$

As to be seen from Eqs. (30) and (31), both h and w depend linearly on the mass m of the pick-up ion. Therefore, it is important to notice that in Titan's equatorial plane, the parameter h determines the extension of the particle trajectory in

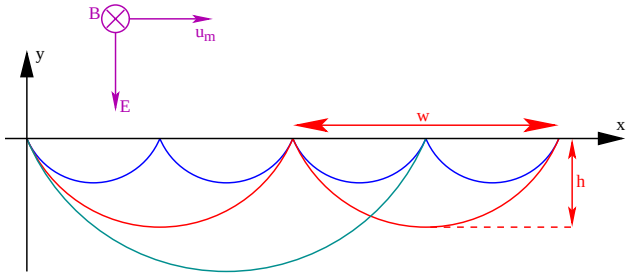

Fig. 2. Schematic illustration of the pick-up process at Titan. The homogeneous ambient plasma flow is directed parallel to the x-axis, whereas the background magnetic field is oriented antiparallel to the z-axis. The sketch shows the cycloidal motion of three ions with different masses which have been inserted into the magnetospheric plasma flow at $\boldsymbol{x}(t{=}0){=}0$, their initial velocity being $\boldsymbol{v}(t{=}0){=}0$. Both the height h and the width w of the cycloidal particle trajectories depend linearly on the mass. This is illustrated for three pick-up ions of mass m (blue), $2m$ (red) and $3m$ (cyan). Due to these differences in the height of the cylcoids, the spatial extension of the ionospheric tail in the direction of the convective electric field depends on the particle mass.

the direction of the convective electric field. Consequently, the extension of the ionospheric tail in the direction of the convective electric field is a measure of the mass of the respective ion species. For three ion species with representative masses, the parameters w and h are listed in Table 1.

4 First step: single-species upstream flow and multi-species ionosphere

In the first step, two additional ionospheric species have been incorporated into the simulation model. The heaviest of the three ionospheric species is molecular Nitrogen ($m\left(N_2^+\right)$ =28 amu), the corresponding production parameters are given in detail by Simon et al. (2006c). Methane has been chosen as the second ionospheric species. On the one hand, it is one of the predominant neutral species (Nagy and Cravens, 1998). On the other hand, its molecular weight ($m\left(CH_4^+\right)$ =16 amu) does not differ significantly from the mass of atomic Nitrogen, being another important constituent of Titan's ionosphere (Keller et al., 1992). In agreement with the model developed by Modolo (2004), molecular Hydrogen ($m\left(H_2^+\right)$ =2 amu) is assumed to be the third component of the model ionosphere. The model does not include interaction processes between ions of different species, such as collisions or charge exchange reactions. Besides, due to the large size of the simulation box, the spatial resolution in the ionosphere region is limited, the diameter of a single cell of the simulation grid being of the order of 400 km. For simplicity, the same production function has been utilized for Nitrogen as well as for Methane and Hydrogen. Of course, this is also quite useful for restricting the numerical complexity of the ionosphere model. This setting is in correspondence to the hybrid study presented by Sillanpää et al. (2006) and recent MHD results discussed by Ma et al. (2006), where the production rates of Methane and molecular Nitrogen are also of at least the same order. Besides, as the discussion will focus on analyzing the global features of Titan's induced magnetotail instead of covering the detailed properties of the ionosphere, such an approach is absolutely justified. Specifically, earlier simulation results clearly illustrate that the global structure of the interaction region is not significantly modified by minor changes in the form of the production function (cf. Bagdonat, 2004; Bößwetter et al., 2004). Of course, for a direct comparison with data from the Cassini plasma spectrometer, both the resolution near the surface and the quality of the ionosphere model would have to be enhanced.

Table 1. Due to the pick-up process, ionospheric ions are moving on cycloidal trajectories in the direction of $\boldsymbol{E}\times\boldsymbol{B}$. For three representative ion species, the table shows the width w and the height h of the cyclodial trajectories, as given by Eqs. (30) and (31). The extensions of the cylcoids are of the same order or even larger than the diameter ofTitan. It can also be seen that, perpendicular to the undisturbed flow direction, the cylcoids are well located inside the simulation boxes, possessing an extension of 7.5 R_T in E^+ direction. The radius of Titan is R_T=2575 km.

Ion species	Molecular weight	Height h	Width w
H_2^+	2 amu	0.4 R_T	1.2 R_T
CH_4^+	16 amu	3.1 R_T	9.8 R_T
N_2^+	28 amu	5.4 R_T	17.1 R_T

To sum up the major idea, the simulations presented in the following will help understand the global features of the interaction between the Saturnian magnetospheric plasma flow with Titan's multi-component ionosphere. Three different species have been selected to represent Titan's ionosphere. The mass of the first species (molecular Nitrogen) is around a factor 3 higher than the mass of the upstream ions, whereas the mass of the second species (Methane) is comparable to that of the magnetospheric particles. Finally, the third ion mass (molecular Hydrogen) is around a factor 5 smaller than the mass of the upstream ions. Thus, the model should provide a general impression of the tail structure arising from a multi-component ionosphere due to the pick-up process. Besides, by means of this approach, it is possible to gain access to the problem of how the magnetic field topology in the vicinity of Titan is affected by the multi-component nature of the ionosphere. Comparison with a study of Titan's ionospheric tail conducted by Luhmann (1996) will allow to validate the simplifying approach presented above.

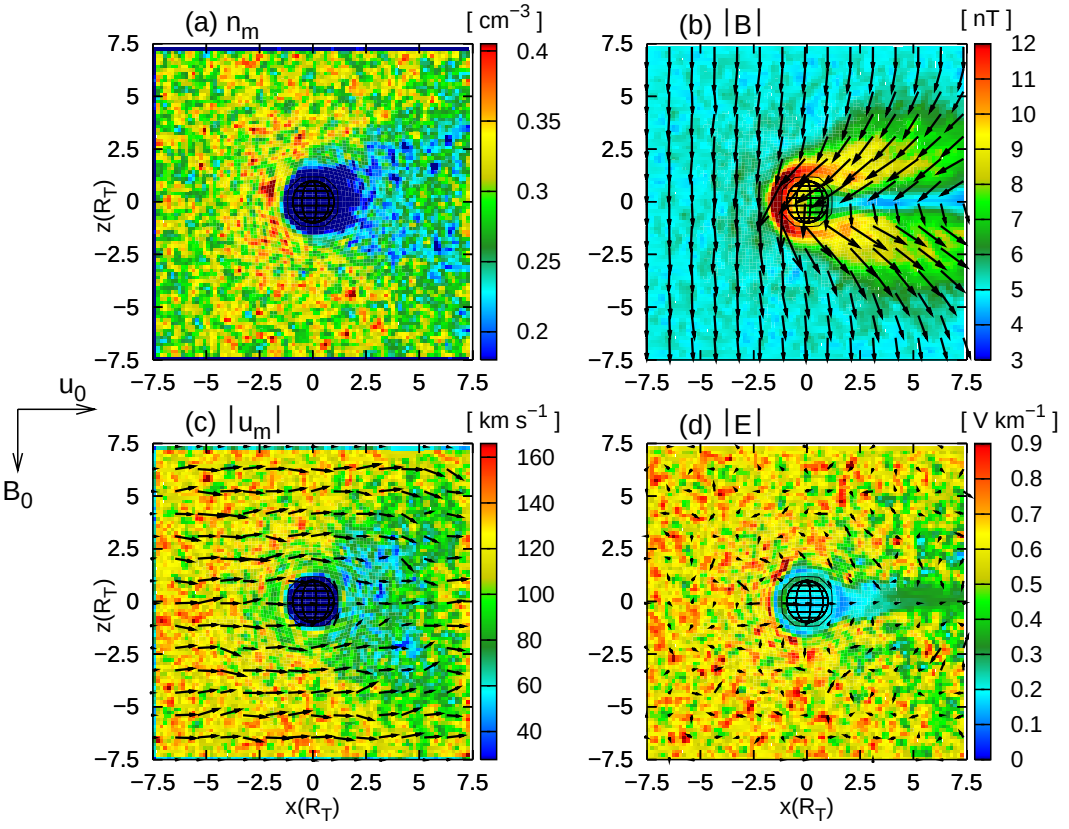

Fig. 3. Titan's plasma environment at 18:00 Saturnian local time. In contrast to the simulations presented by Simon et al. (2006c,b), the ionosphere is assumed to be consisting of three different species. The figure displays **(a)** the magnetospheric plasma density, **(b)** the magnetic field strength, **(c)** the magnetospheric plasma velocity and **(d)** the electric field strength for a cut through the polar plane, coinciding with the (x, z) plane of the coordinate system. Both the magnetospheric plasma parameters and the electromagnetic field configuration are quite similar to the results obtained by using a two-species code, i.e. these quantities are not affected by the incorporation of two additional ionospheric species into the simulation model.

In the following discussion, the three ionospheric species are denoted by the subscripts 1 (Nitrogen), 2 (Methane) and 3 (Hydrogen).

4.1 General features

For a cut through Titan's polar plane, Fig. 3 displays the magnetospheric plasma density as well as the electromagnetic fields. The ionospheric densities and velocities for the same cutting plane are shown in Fig. 4. Figures 5 and 6 display the plasma parameters and the electromagnetic field quantities for a cut through the (x, y) plane of the coordinate system, being identical to Titan's equatorial plane. In the following discussion, the hemisphere where the undisturbed convective electric field is pointing towards Titan will be referred to as the E^- hemisphere, whereas the hemisphere where the electric field is directed away from the obstacle is called the E^+ hemisphere. Thus, in the 18:00 local time scenario, the $(y>0)$ hemisphere is identical to the E^- hemisphere, while the $(y<0)$ hemisphere corresponds to the E^+ hemisphere. In other words, the E^- hemisphere is always the side of Titan that faces Saturn.

As to be seen from Fig. 3, the situation in the polar plane is quite similar to the results obtained by using a single-species ionosphere model. Neither the magnetospheric plasma density nor the velocity is dramatically affected by the presence of the obstacle[1], i.e. only a slight reduction of both the magnetospheric ion density and velocity manifests in the downstream region. Besides, the magnetic draping pattern remains nearly unaffected by extending the complexity of the ionosphere model. In agreement with the results presented by Simon et al. (2006c), the magnetic lobes are still confined to a region with a diameter of around $\pm 3\,R_T$ perpendicular to the direction of the undisturbed flow. The peak field strength achieved at Titan's dayside as well as the magnetic field enhancement in the lobes have almost the same values as in the two-species results. The magnetic field topology in the vicinity of Titan arises mainly from the transport of the field

[1]The reason for this phenomenon will be revealed when the upstream plasma flow is split up in two species with different masses.

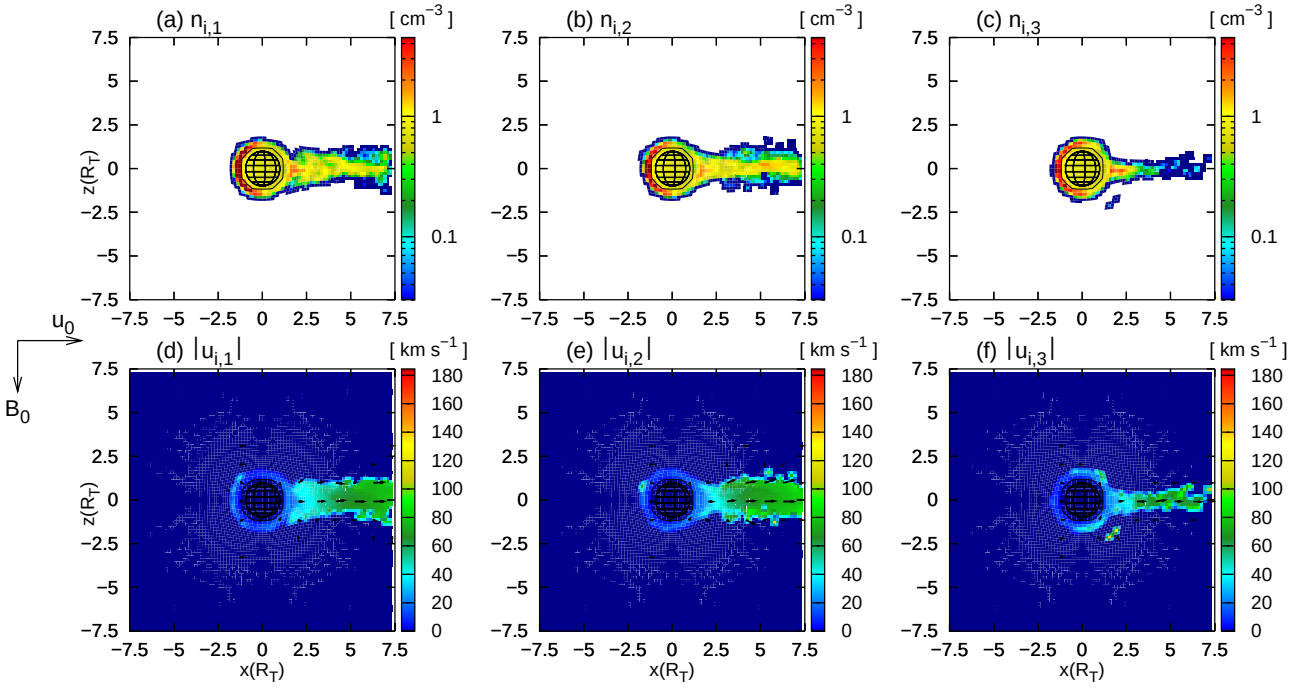

Fig. 4. Titan's plasma environment at 18:00 Saturnian local time. The figure shows the ionospheric plasma parameters for a cut through Titan's polar plane. **(a)** and **(d)** display the mean density $n_{i,1}$ and velocity $u_{i,1}$ of molecular Nitrogen (N_2^+) ions, whereas **(b)** and (e) show the same parameters for the Methane (CH_4^+) component of the ionosphere. The density and velocity of the lightest ionospheric species, molecular hydrogen (H_2^+), are displayed in **(c)** and **(f)**. Each of these species forms a narrow tail downstream of the obstacle. At least in the polar plane, no significant difference manifests in the tail structures of ions of different masses.

lines by the plasma flow. Due to the ionospheric ion density in the magnetic lobe regions being negligible, the convection of the field lines along the flow is primarily governed by the magnetospheric plasma, i.e. the convective electric field can be expressed as

$$\begin{aligned} \boldsymbol{E}_c &= -\Bigg(\frac{n_m}{n_m + \sum_{k=1}^{3} n_{i,k}}\boldsymbol{u}_m + \\ &\quad + \sum_{j=1}^{3} \frac{n_{i,j}}{n_m + \sum_{k=1}^{3} n_{i,k}}\boldsymbol{u}_{i,j}\Bigg) \times \boldsymbol{B} \\ &\approx -\boldsymbol{u}_m \times \boldsymbol{B} \quad . \end{aligned} \tag{32}$$

The change $\partial_t \boldsymbol{B}$ of magnetic field strength arising from this term can therefore be written as

$$\frac{\partial \boldsymbol{B}}{\partial t} = \nabla \times (\boldsymbol{u}_m \times \boldsymbol{B}) \quad , \tag{33}$$

i.e. the magnetic field dynamics in the lobe regions are almost entirely controlled by the magnetospheric plasma. As the magnetospheric flow remains almost unaffected by the modification of the ionosphere model, the magnetotail structures obtained from the different simulation approaches are almost identical. As to be seen in Fig. 4, in the downstream region, each of the three ionospheric species forms a narrow tail. Except for the particle density $n_{i,3}$ in the H_2^+ tail being around a factor 5 smaller, in the polar plane, the overall tail structure of the three species is nearly identical.

In strong analogy to the results shown by Simon et al. (2006c,b), a pronounced magnetic pile-up region is formed at Titan's dayside. As to be seen from Fig. 5b, the region of enhanced magnetic field strength is asymmetric with respect to the direction of the electric field. The major reason for the formation of this structure is the incapability of the magnetic field to penetrate the dayside ionosphere region. In the immediate vicinity of Titan's dayside, the ionospheric particles become predominat, i.e. the convective electric field can be expressed as

$$\begin{aligned} \boldsymbol{E}_c &= -\Bigg(\frac{n_m}{n_m + \sum_{k=1}^{3} n_{i,k}}\boldsymbol{u}_m + \\ &\quad + \sum_{j=1}^{3} \frac{n_{i,j}}{n_m + \sum_{k=1}^{3} n_{i,k}}\boldsymbol{u}_{i,j}\Bigg) \times \boldsymbol{B} \\ &\approx -\sum_{j=1}^{3} \frac{n_{i,j}}{\sum_{k=1}^{3} n_{i,k}}\boldsymbol{u}_{i,j} \times \boldsymbol{B} \quad . \end{aligned} \tag{34}$$

As the velocity of the newly generated ionospheric particles almost vanishes – in fact, these particles are inserted into the simulation domain with an initial velocity of $\boldsymbol{v}_i$=0, – the convective electric field near Titan's dayside is almost

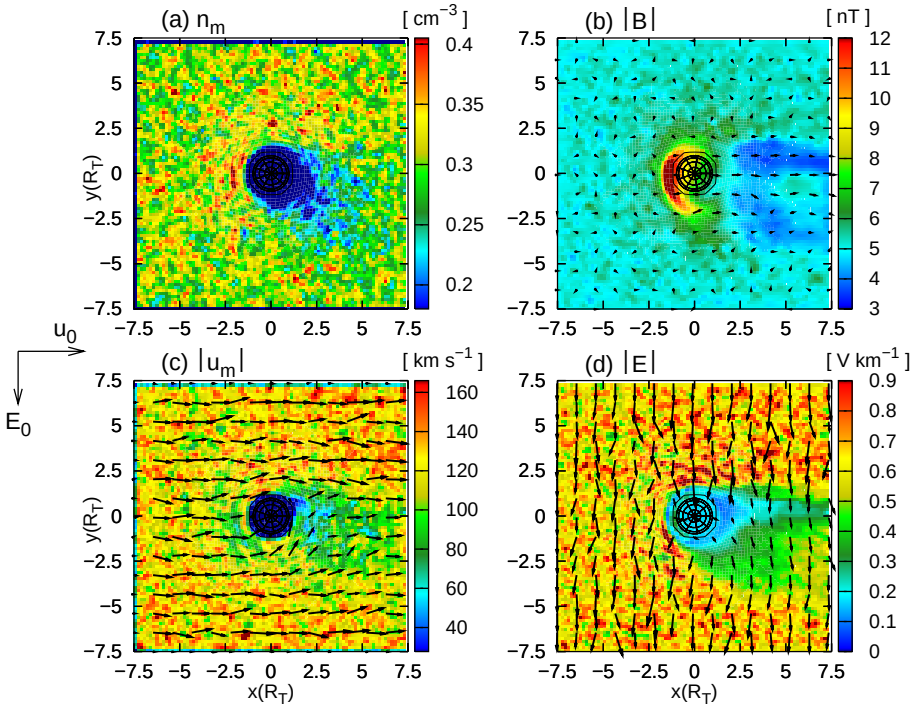

Fig. 5. Titan's plasma environment at 18:00 Saturnian local time. In analogy to Fig. 3, the figure displays the magnetospheric plasma parameters and the electromagnetic fields for a cut through the (x, y) plane which is identical to Titan's orbital plane. As the formation of the magnetic pile-up region at Titan's dayside is mainly governed by the field convection along the magnetospheric plasma flow, the magnetic field signature in the vicinity of Titan is very similar to the results obtained by using a single-species ionosphere model.

zero. Despite the relatively rough spatial resolution in the immediate vicinity of the obstacle, a region of reduced electric field strength at the dayside can be clearly identified in Fig. 5d. Hence, the change of magnetic field strength inside the ionosphere region almost vanishes, so that the field lines are pressed against the obstacle and a pile-up region is formed. As to be seen from Fig. 6e, in the dayside ionosphere region, even the density of a single ionospheric species is around a factor 5/0.3=16.7 higher than the ambient magnetospheric plasma density. Thus, according to Eq. (34), the presence of a single ionospheric species is absolutely sufficient for preventing the magnetic field lines from penetrating the ionosphere. Consequently, the structure of the magnetic pile-up region at Titan's dayside is not affected by the incorporation of two additional ionospheric species into the model. This is the reason why the magnetic signatures obtained with the two-species model are almost identical to the situation displayed in Fig. 5b.

As to be seen from Fig. 6, each of the three ionospheric tails exhibits a strong asymmetry with respect to the direction of the convective electric field. However, it is also obvious that the tail extension in the E^+ hemisphere differs significantly for the three species. This effect depends on the mass of the respective ion species and is in complete agreement with the analytical discussion given in the previous section. On the one hand, according to Eq. (30), the height h of the cycloidal particle trajectories for molecular Nitrogen ions is given by

$$h_{N_2^+} = 2\frac{u_m m}{e|B|} \approx 2\frac{120\ \mathrm{km/s} \cdot 28 m_p}{e \cdot 5\ \mathrm{nT}} = 5.4\, R_T \quad , \qquad (35)$$

where the undisturbed upstream values given by Neubauer et al. (1984) have been used. As displayed in Fig. 6a, in a distance of about 5.5 R_T perpendicular to the undisturbed flow direction, the Nitrogen density in the tail is comparable to or even larger than the ambient magnetospheric plasma density. On the other hand, the orientation of the tail with respect to the direction of $\boldsymbol{E}$ is also in complete correspondence to the theroretical discussion (cf. Fig. 2).

The mass of Methane ions is around a factor 1.75 smaller than the molecular weight of N_2^+. Therefore, the ionospheric tail of this species should possess an extension of about

$$h_{CH_4^+} \approx \frac{5.4\, R_T}{1.75} = 3.1\, R_T \qquad (36)$$

in the direction of the electric field. As to be seen from Fig. 6b, ionospheric Methane ions can be found in distances below 2.7 R_T perpendicular to the x-direction. As both the velocity and the magnetic field strength in the area covered by the Methane tail differ from the undisturbed upstream values, the simulation results are in reasonable agreement with the theoretical prediction.

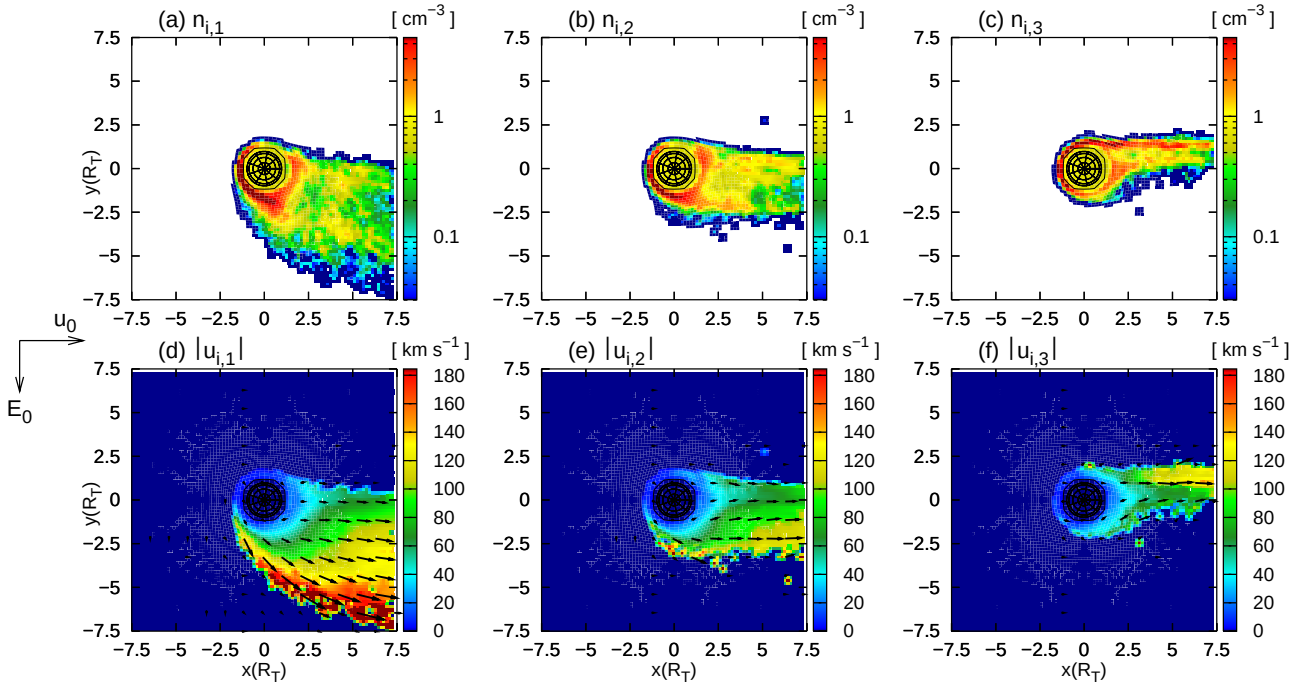

Fig. 6. Titan's plasma environment at 18:00 Saturnian local time. The figure shows the ionospheric plasma parameters for a cut through Titan's equatorial plane. Specifically, the figure displays the densities **(a)** of molecular Nitrogen ions, **(b)** of Methane ions and **(c)** of molecular Hydrogen ions. The corresponding plasma velocities are shown in panels **(d–f)**. As the convective electric field at the tail's Saturn-facing flank is perpendicular to the tail and points inside the tail, each of the three ionospheric species is confined to the anti-Saturn facing E^+ hemisphere. The particles are moving on cycloidal trajectories, their extension h in the direction of the convective electric field depending linearly on the ion mass (Mass Spectrometer Effect).

Finally, the tail developed by the molecular Hydrogen ions shall be investigated. As to be seen from Fig. 6c, the particles of this species are definitely forbidden to enter the Saturn-facing hemisphere of Titan. Besides, it is important to notice that significant Hydrogen densities can be found only in a narrow tail region between $y \geq 0$ and $y \leq 1.5\, R_T$. Setting both the magnetic field strength and the magnetospheric plasma velocity on the undisturbed upstream values yields a height of

$$h_{H_2^+} \approx \frac{3.1\, R_T}{8} = 0.4\, R_T \tag{37}$$

for the cycloidal particle trajectories. Thus, the tail developed by the Hydrogen ions is practically not shifted in the direction of the convective electric field. Since the plasma velocity directly beyond Titan is around a factor 1.5 smaller than the upstream value of u_0=120 km/s (cf. Fig. 5c) and the magnetic field strength also differs from the homogeneous background value, the deviation of the analytical value from the simulation result is absolutely expectable. Assuming a field strength of $B \approx 4$ nT and a mean plasma velocity of around u_m=80 km/s in the tail region (cf. Figs. 5c and d) yields a height of

$$\tilde{h}_{\mathrm{H}_2^+} \approx \frac{5}{6} h_{\mathrm{H}_2^+} \tag{38}$$

which is almost identical to the value obtained from the homogeneous upstream parameters. Besides, one should keep in mind that the theoretical estimation of the tail extensions presented in the previous section is based on the simplifying assumption of a point-like ion source.

In general, due to their large gyroradii, the cycloidal trajectories of the newly generated Nitrogen ions traverse almost entirely those regions of the E^+ hemisphere where neither the magnetic field strength nor the mean magnetospheric plasma velocity is significantly affected by the presence of the obstacle. For this reason, best agreement between theoretical calculations and the simulation results could be achieved for the Nitrogen ions. In other words, the larger is the mass of an ionospheric ion species, the more adequate is the simplified analytical model of a point-like source in a homogeneous flow for covering the motion of these newly generated particles in the equatorial plane.

4.2 Titan's ionospheric tail: a natural ion mass spectrometer!

The spatial dispersion of the pick-up ion trajectories in Titan's ionospheric tail has also been investigated by Luhmann (1996) who has applied a simple test particle model to the situation during the Voyager 1 flyby. In complete agreement

with the simulation results presented in the previous section, Luhmann (1996) predicts the formation of a broad and highly asymmetric wake in which ion species of different masses become spatially dispersed. It is also demonstrated that the ionospheric wake region significantly exceeds the region that is covered by the magnetic field distortions in the near-Titan region. Due to the spatial dispersion of different ion species, Luhmann (1996) suggests that Titan's ionospheric tail may be considered a *natural ion mass spectrometer*. In agreement with the hybrid simulation results, it is illustrated that light Hydrogen ions are confined to the magnetospheric plasma flow wake directly beyond Titan, whereas the heavier ions move on cycloidal trajectories in Titan's equatorial plane, the extension of the cyloids in the direction of the convective electric field depending on their masses. Thus, a spacecraft flying to Titan's ionospheric wake should be able to detect a sequence of ion beams of different masses. The ion flux in each of these beams should be a direct measure for the ion production rate as well as for the corresponding neutral density of the respective species. The results of the study conducted by Luhmann (1996) have shown to be completely reproducible in the framework of the hybrid model. As Luhmann (1996) has also found evidence for the occurence of such a mass spectrometer effect in the data obtained by Voyager 1, it is absolutely reasonable to expect the formation of such a spatially dispersive tail structure, at least in the case of sufficiently homogeneous ambient magnetospheric conditions. If Titan's plasma environment is highly perturbed due to local magnetospheric variations, it is likely that the formation of the mass spectrometer is suppressed and therefore, a clear distinction between different species is no longer possible.

4.3 Multi-species versus single-species ionosphere model

Due to the height of their cycloidal trajectories being largest, the extension of the ionospheric N_2^+ tail in the direction of the electric field exceeds the tail diameters of the two lighter species. Therefore, the N_2^+ ions also determine the extension of the cavity in the electric field strength, being characteristic for the field topology in the equatorial plane. The trajectories of newly generated CH_4^+ and H_2^+ ions are almost completely located in this electric field cavity and consequently, the pick-up force acting on these ions is significantly weaker than the force on the Nitrogen ions. Thus, as displayed in Figs. 6d–f, the velocity of the Nitrogen ions at the tail's anti-Saturn-facing flank exceeds the maximum velocity of both other species by almost a factor of 2 and is even significantly larger than the upstream magnetospheric flow velocity. Although the CH_4^+ and H_2^+ ions are lighter than the molecular Nitrogen particles and hence, even a reduced Lorentz force should be able to give rise to an acceleration that is comparable to the effect on the N_2^+ ions, the CH_4^+ and H_2^+ velocity near the tail's flank in the E^+ hemisphere does not match the N_2^+ velocity. For this reason, the pick-up process of the light ionospheric species is slowed down by the heavy ones.

In any case, the major features of the electric field topology in the equatorial plane seem to be determined by the heaviest ionospheric species, for their gyration trajectories possess the largest extension. Since the tails of the lighter species – e.g. CH_4^+ and H_2^+ – are completely located inside the area covered by the N_2^+ tail, they are unable to alter the extension of the electric field cavity. Of course, if the two-species hybrid simulations presented by Simon et al. (2006c) had contained molecular Hydrogen or Methane instead of molecular Nitrogen as the only ionospheric species, an additional incorporation of the heavy N_2^+ ions would have gone along with a widening of the cavity in the electric field strength. Therefore, if a simulation model is meant to provide a global picture of the electric field structure in the vicinity of Titan, it is sufficient to include the heavy ionospheric species, such as molecular Nitrogen. The incorporation of relatively light ions like Methane or Hydrogen is mandatory for covering the ionospheric mass-spectrometer effect, but cannot significantly alter the electric field topology. Besides, the major feature of the magnetic draping pattern have also proven to be completely covered in the framework of the two-species model.

These aspects are also illustrated in Fig. 7. For the case of Titan's dayside being exposed to the upstream plasma flow, the figure displays the situation in the equatorial plane when Methane ions (CH_4^+) are the only species of ionospheric origin that is taken into consideration. Compared to the runs with both a Methane and a molecular Nitrogen component, the diameter of the electric field cavity has clearly diminished, since the gyroradii of Methane ions are smaller than those of molecular Nitrogen. In addition, the peak velocity that is achieved in the anti-Saturn-facing pick-up region is comparable to the value achieved by the N_2^+ ions in the multispecies simulations. As to be seen in Fig. 7e, even in the central ionospheric tail region beyond Titan, the mean velocity of the pick-up flow is about a factor of 1.5 higher than in the Methane tail that is developed when the ionosphere is also consisting of molecular Nitrogen. This clearly illustrates that the pick-up process of the lighter species is *enslaved* by the heaviest one. Of course, a major condition for such a behaviour is that the procuction rates and therefore the number densities of light and heavy species are of the same order of magnitude. If, for instance, the production rate of heaviest species is so small that the dynamics of these particles are governed by a simple test-particle model, these ions will neither affect the electromagnetic field topology nor the pick-up process of the lighter ions.

Hence, in the case of a multi-species ionosphere, the heavy Nitrogen ions form an extended tail in the E^+ hemisphere and, at the outer flank of this tail, achieve a velocity that even exceeds the magnetospheric flow velocity by a factor of 2. However, directly beyond Titan, the formation of this tail goes along with the development of a region denoted by a

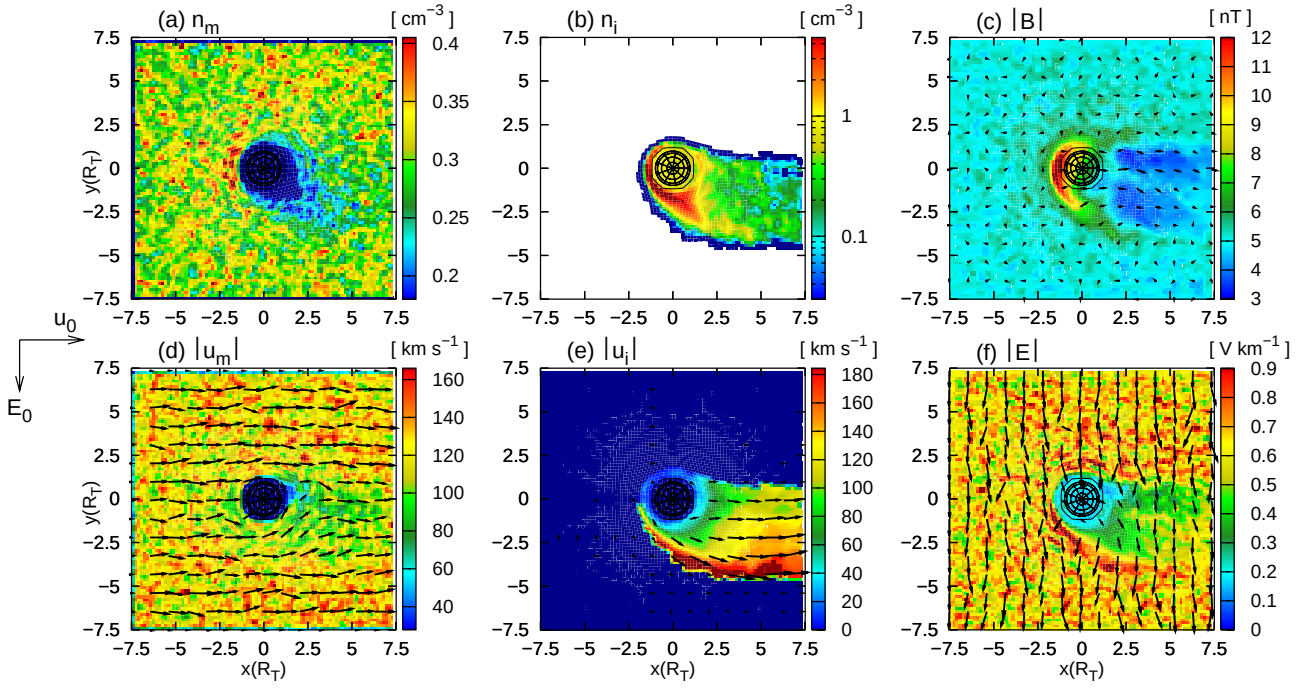

Fig. 7. Titan's plasma environment at 18:00 local time. The figure displays a cut through the equatorial plane for the case of Methane being the only species of ionospheric origin. Compared to the case of a multi-species ionosphere, the peak ionospheric velocity u_i that is achieved in the E^+ hemisphere is about a factor of 2 higher.

reduced electric field strength. Due to their small masses, the newly generated Methane and molecular Hydrogen ions are developing a tail structure that is completely located in the electric field cavity. Therefore, they experience a reduced pick-up force and are unable to match the high velocities at the outer flank of the N_2^+ tail. Since in the case of an ionosphere that is consisting only of CH_4^+, the Methane ions are able to achieve a noticeably higher velocity (cf. Fig. 7), it is obvious that the heavy ionospheric species affect the pick-up process of the lighter ones.

5 Second step: multi-species upstream flow and multi-species ionosphere

The previous section dealt with the analysis of Titan's plasma environment by means of a hybrid model that considers the multi-component nature of the obstacle's ionosphere. It has been demonstrated that on the one hand, neither the magnetospheric plasma parameters nor the electromagnetic field quantities are significantly affected by such an extension of the model. On the other hand, the necessity of taking into account several different ionospheric species has been clearly demonstrated as the structure of the ionospheric tail, i.e. its extension in the direction of the electric field, depends on the mass of the particles. However, the most critical issue that has remained in the model is the approximation of the ambient magnetospheric plasma conditions by using a single ion species. Of course, average values have been chosen for both the mass and the charge of these particles (see also Kabin et al., 1999, 2000; Kallio et al., 2004; Sillanpää et al., 2006) and therefore, the results should provide an adequate impression of the global magnetospheric plasma signatures in the vicinity of Titan. Nevertheless, according to Voyager 1 data, the plasma flow that impinges on Titan's ionosphere consists of two major species: atomic Nitrogen (N^+) and Hydrogen (H^+) ions. At a certain position, both species experience the same electromagnetic fields, and consequently, the same Lorentz force is acting on magnetospheric ions of different species. However, due to the mass of Hydrogen ions being around a factor 14 smaller than the mass of Nitrogen, the *acceleration* of the H^+ particles should be about one order of magnitude larger than the modification of the N^+ particle trajectories. It must therefore be expected that the plasma densities and velocities of the two species develop significantly different features. This aspect of Titan's plasma interaction will be adressed in the following. Of course, the simulations will also retain the multi-species nature of Titan's ionosphere.

It is interesting to notice that, even though the temperature of the Hydrogen component is of the order of $k_B T_{H^+}$=210 eV and is therefore around a factor 2900 eV/210 eV≈14 smaller than the temperature of the Nitrogen ions (Neubauer et al., 1984; Backes, 2005), the mean

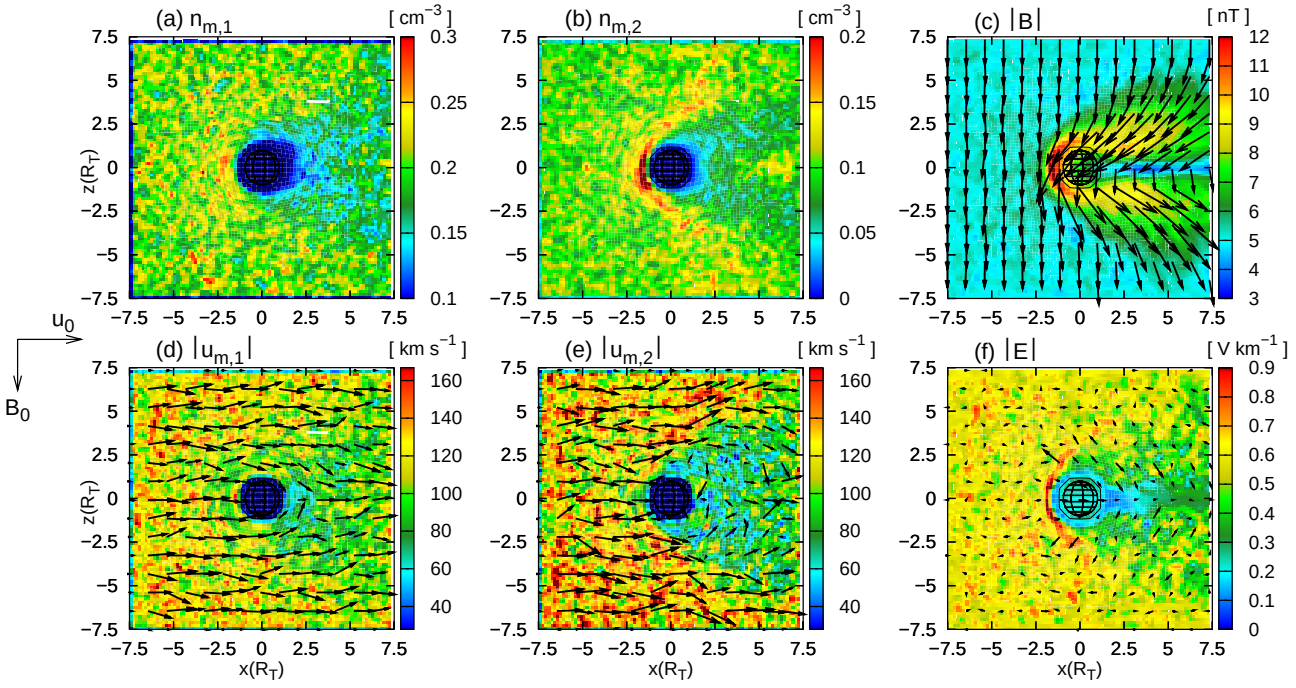

Fig. 8. Titan's plasma environment at 18:00 local time. On the one hand, the multi-species nature of the ionosphere has been retained, but on the other hand, the magnetospheric plasma flow is now represented by two distinct ion species. For a cut through the polar plane, the figure displays **(a)** the magnetospheric N^+ density $n_{m,1}$, **(b)** the magnetospheric H^+ density $n_{m,2}$, **(c)** the magnetic field, **(d)** the mean N^+ velocity $u_{m,1}$, (e) the mean H^+ velocity $u_{m,2}$ and **(f)** the electric field strength. The heavy Nitrogen ions behave similar to the hypothetical (N^+/H^+) ions that have represented the magnetospheric plasma flow in earlier simulations carried out by Simon et al. (2006c), since the masses of these two species differ only by a factor of 1.5.

thermal velocities

$$v_{\mathrm{th}} = \sqrt{\frac{3k_B T}{m}} \tag{39}$$

of both species are almost identical. Due to the mass of the Hydrogen ions being about a factor 14 smaller than the mass of atomic Nitrogen, the mean thermal velocity of H^+ reads

$$v_{\mathrm{th,H^+}} = \underbrace{\sqrt{\frac{210}{2900}} \cdot 14}_{\approx 1} v_{\mathrm{th,N^+}} \approx v_{\mathrm{th,N^+}} \quad . \tag{40}$$

Since the mean velocity value

$$v_{\mathrm{th,H^+}} \approx v_{\mathrm{th,N^+}} \approx 244\,\mathrm{km/s} \tag{41}$$

is around a factor 2 higher than u_0=120 km/s, the dynamics of both the Hydrogen and the Nitrogen ions are governed by nondirectional thermal motion. The hypothetical (N^+/H^+) ions used in simulations with a single-species representation of the magnetospheric plasma flow featured the same property.

In the following sections, the simulation results obtained with this multispecies code will be presented. Two cases shall be compared: On the one hand, the case of Titan's dayside being exposed to the upstream flow at 18:00 LT will be analyzed. This situation will be directly compared to the case of the upstream flow interacting with Titan's nightside ionosphere at 06:00 LT. Besides, a comparative discussion of the different simulation approaches will be given, emphasizing the importance of the high thermal velocity of the light H^+ ions. In all figures presented in the following section, the magnetospheric ion species will be denoted by the subscripts $m, 1$ (Nitrogen) and $m, 2$ (Hydrogen). The notation that is used for distinguishing between the three species of ionospheric origin is the same as in the previous section.

5.1 18:00 Saturnian local time

The simulation results for the case of Titan's dayside being exposed to the upstream plasma flow are presented in Figs. 8–11. Figure 8 displays the magnetospheric plasma parameters and the electromagnetic fields for a cut through the polar plane, coinciding with the (x, z) plane of the coordinate system. The ionospheric plasma densities and velocities for the polar plane are shown in Fig. 9. For a cut through Titan's orbital plane, the magnetospheric and ionospheric parameters as well as the field quantities are displayed in Figs. 10 and 11, respectively.

As to be seen from Figs. 8a and d, the signatures developed by the heavier magnetospheric species N^+ in the polar

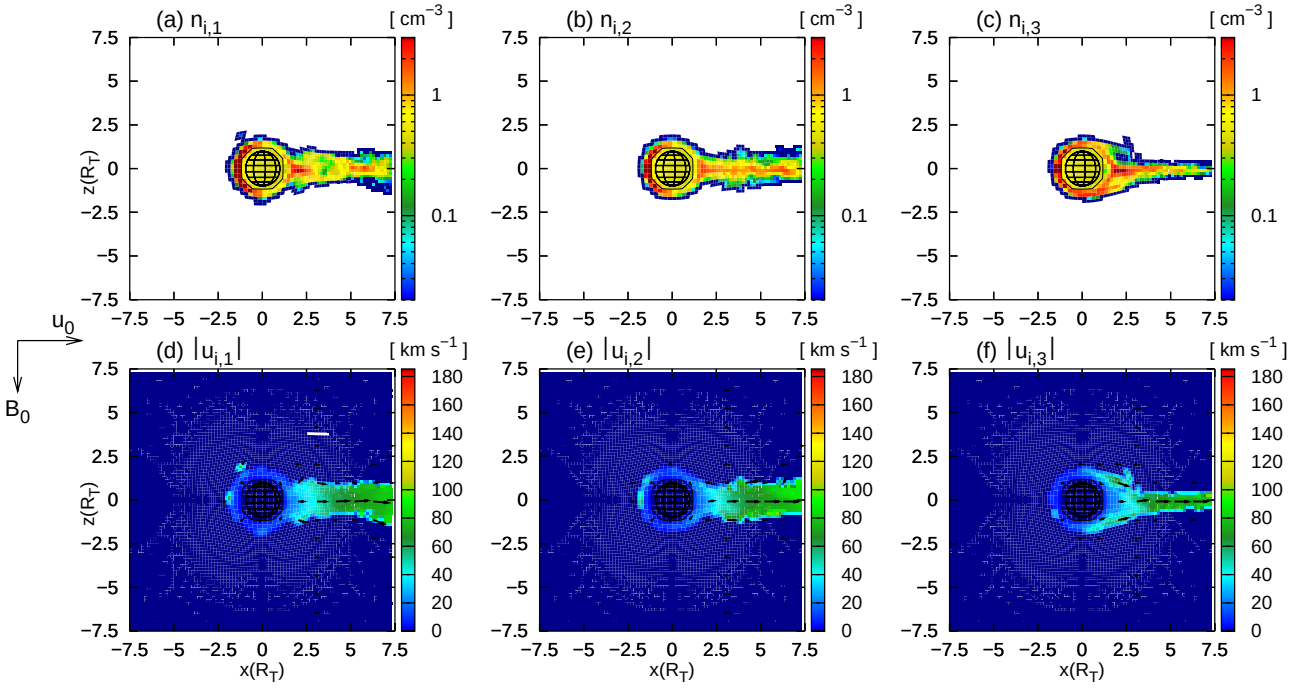

Fig. 9. Five-species simulation of Titan's plasma environment at 18:00 local time – Ionospheric plasma parameters. For a cut through the polar plane, the figure displays the densities of **(a)** molecular Nitrogen, **(b)** Methane and **(c)** molecular Hydrogen. The corresponding velocities are shown in **(d–f)**, respectively. Each of the three species forms a narrow tail downstream of the obstacle. The tail structure corresponds to the results obtained from the more simplifying single-species ionosphere model. Due to the small velocity of the ionospheric ions, a narrow cavity of reduced electric field strength is formed directly beyond the obstacle.

plane feature many similarities to the results obtained by assuming the upstream flow to consist only of a single species (cf. Sect. 4). Obviously, a slightly pronounced cavity of reduced N^+ plasma density arises downstream of the obstacle, the particle density being around a factor 0.7 smaller than in the undisturbed upstream flow. In the same region, the velocity $u_{m,1}$ decreases from values around 120 km/s to a velocity of only 80−90 km/s. This weak reaction of the Nitrogen component on the presence of the obstacle is in complete correspondence to the interaction of a single-species flow with Titan's ionosphere, as discussed in Sect. 4. This analogy is absolutely expectable for the mass of Nitrogen ions differs only about a factor of 1.5 from the mass of the hypothetical (N^+/H^+) ion species that has been applied to represent the impinging magnetospheric plasma flow. In other words, at a certain position in the simulation box, a Nitrogen ion and a hypothetical (N^+/H^+) ion experience the same Lorentz force as well as, due to their masses being of the same order, the same acceleration

$$\ddot{\boldsymbol{x}} = \frac{e}{m}\left(\boldsymbol{E} + \boldsymbol{v} \times \boldsymbol{B}\right) \quad . \tag{42}$$

Hence, the global topology of the plasma paramaters should exhibit an almost similar structure.

However, the mass of the second upstream species H^+ is one order of magnitude smaller than the mass of the hypothetical (N^+/H^+) particles. Moreover, in the scenario under consideration, the mass of the Hydrogen ions is about a factor 14 smaller than the mass of the other upstream species N^+. At a certain position, a Hydrogen particle experiences the same electromagnetic fields as a Nitrogen particle and hence, the Lorentz force acting on both ions is of the same strength. However, as expressed by Eq. (42), the acceleration of the Hydrogen ion is around a factor 14 larger. Therefore, as can be seen in Figs. 8b and e, in the vicinity of Titan, the plasma parameters of this species undergo a noticeable modification. The Hydrogen particles are clearly deflected around the obstacle, giving rise to a cone-shaped region of slightly reduced Hydrogen density in the downstream region. In contrast to the velocity of the Nitrogen component, the velocity vectors of the Hydrogen flow are noticeably distorted near the flanks of the tail; i.e. these particles are guided along the flanks of the cone-like region and are at least partially forbidden to penetrate this structure. As the Hydrogen ions are pressed against the outer flanks of the magnetotail when entering the vicinity of Titan, the interaction leads to the formation of a parabolically shaped area of slightly enhanced Hydrogen density that is surrounding the H^+ wake. This structure is clearly identifiable near the dayside of the obstacle (cf. Fig. 8b).

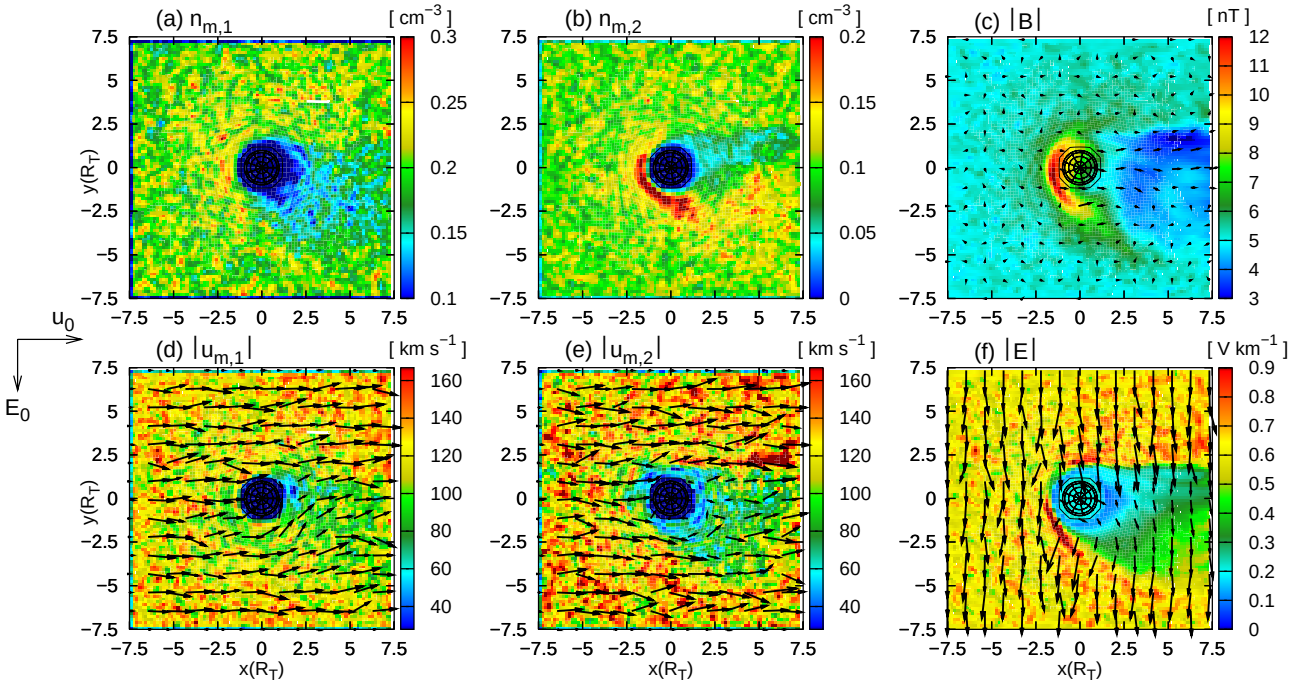

Fig. 10. Five-species simulation of Titan's plasma environment at 18:00 local time – Magnetospheric plasma parameters and electromagnetic fields in the equatorial plane. The figure displays the N^+ density and velocity: **(a)** and **(d)**, the H^+ density and velocity: **(b)** and **(e)**, and the electromagnetic fields: **(c)** and **(f)**. In the E^+ hemisphere, a certain fraction of the light Hydrogen ions is clearly incapable of gaining access to the central tain region, i.e. these particles are moving along the outer flank of the electric field cavity that forms an angle of about 45° with the (+x)-direction.

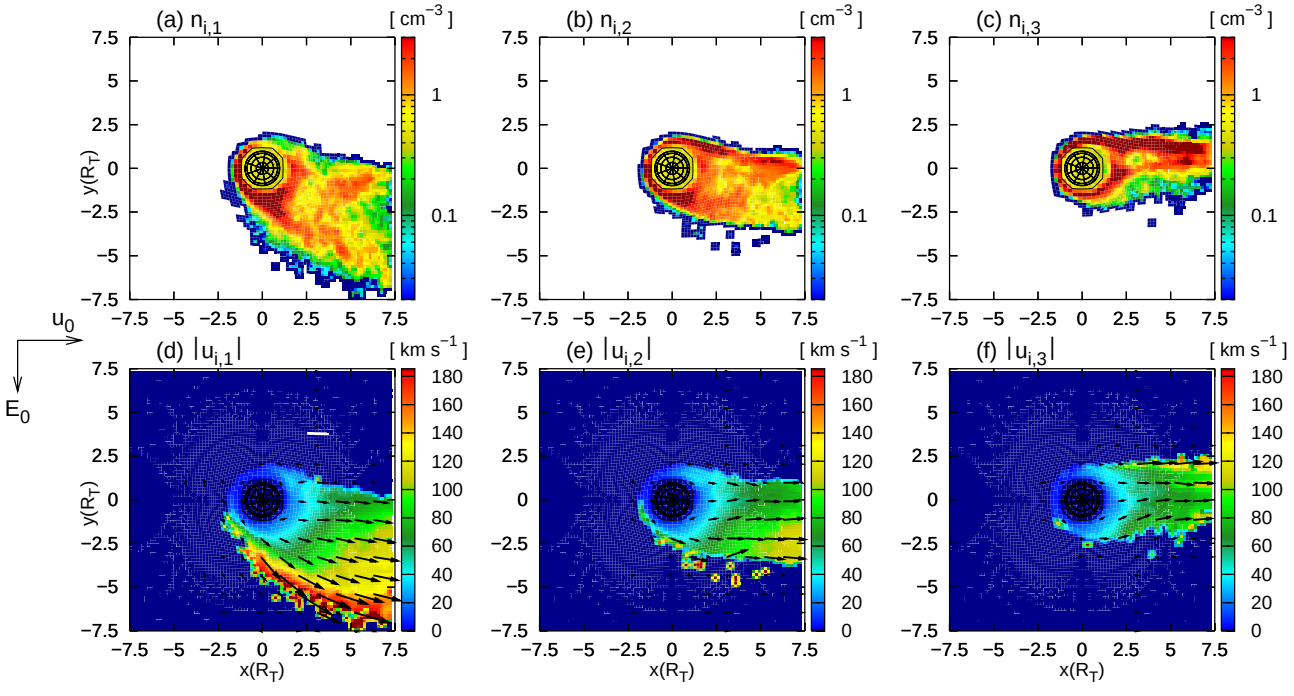

Fig. 11. Five-species simulation of Titan's plasma environment at 18:00 local time – Ionospheric densities and velocities in the equatorial plane. The figure displays the density and velocity of molecular Nitrogen: **(a)** and **(d)**, Methane: **(b)** and **(e)**, and molecular Hydrogen: **(c)** and **(f)**. The mass-spectrometer effect in the ionospheric tail structure is clearly identifiable.

The increase of Hydrogen density in the polar plane arises from the incapability of a certain amount of Hydrogen particles to enter the tail region, so that these ions are pressed against and deflected around the outer boundary of the central tail, denoted by the outer boundary of the magnetic draping pattern. Due to the electron pressure terms, this slight density enhancement goes along with the formation of electric fields that are directed radially away from the obstacle, as to be seen in Fig. 8f. Since the velocity of the ionospheric ions in the tail region (cf. Figs. 9d–f) almost vanishes, their contribution to the convective electric field is practically negligible. Consequently, the electric field strength in the polar plane achieves its minimum value directly beyond the obstacle where the magnetospheric ion densities are smallest.

The velocity plots of Nitrogen and Hydrogen for the polar plane (cf. Fig. 8) clearly illustrate that the smaller is the mass of an impinging ion species, the more significant is the deflection that the respective particles experience in the vicinity of the obstacle. Thus, in analogy to the ionospheric tail, the magnetospheric plasma flow in the vicinity of Titan exhibits some kind of *mass spectrometer effect*. The light upstream species is at least partially incapable of gaining access to the central tail region, whereas only a slight reduction of Nitrogen density occurs. This *magnetospheric ion mass spectrometer* should at least allow a rough distinction between heavy and light upstream ions for the latter ones should not be predominant in the central tail beyond the obstacle. In contrast to the ionospheric ion mass spectrometer, this effect should be observable in the polar plane which is directed perpendicular to the convective electric field. Besides, the mechanism that leads to the partial separation of Nitrogen and Hydrogen ions is quite different to the distinguishment between different ionospheric species, the width of their cycloidal pick-up trajectories depending on the particle masses. In any case, a critical issue is the extremely high thermal velocity of the magnetospheric ions. The extent to which this aspect takes influence on the Hydrogen and Nitrogen tail structures and the spectrometer phenomenon will be investigated in the following section.

The magnetic draping pattern in the polar plane (cf. Fig. 8c) resembles the field topology obtained from the simulation runs with a single upstream species, except for minor changes in the maximum value that is reached in the dayside pile-up region. Besides, in the five-species model, the extension of the magnetic lobes perpendicular to the undisturbed upstream flow direction is lightly increased. Generally, the region of noticeable magnetic field enhancement in the lobes possesses an extension of about $\pm 5\,R_T$ perpendicular to the flow direction, whereas in the simulations presented in the previous section, the same structure covered an area with a diameter of only $\pm 4\,R_T$. When extending the upstream plasma model to multi-species conditions, a slight modification of the magnetic topology is absolutely expectable because the convection of the field lines along the flow is described by the expression

$$\frac{\partial \boldsymbol{B}}{\partial t} = \nabla \times \left[\left(\frac{n_{m,1}}{n_{m,1}+n_{m,2}} \boldsymbol{u}_{m,1} + \right. \right. \\ \left. \left. + \frac{n_{m,2}}{n_{m,1}+n_{m,2}} \boldsymbol{u}_{m,2} \right) \times \boldsymbol{B} \right] \quad , \tag{43}$$

i.e. the formation of the magnetic draping pattern is governed by the dynamics of both upstream species. The Nitrogen component behaves similar to the hypothetical $\left(N^+/H^+\right)$ ions, i.e. in the entire interaction region, the bulk velocity is almost parallel to the positive x-axis. In contrast to this, the H^+ bulk velocity is significantly modified by the deflection of this species around the central tail region. Of course, due to the upstream N^+ density being around a factor 2 higher than the density of H^+, the draping mechanism is still mainly governed by the heavier Nitrogen ions, behaving quite similar to the single-species (N+/H+) upstream plasma. Nevertheless, in regions of high H^+ density - for instance, near the outer flanks of the cone-like wake region, the Hydrogen density may become comparable to the density of N^+, enhancing the influence of the term that depends on $\boldsymbol{u}_{m,2}$ (cf. Eq. 43). Because near the flanks of the wake region, $\boldsymbol{u}_{m,2}$ deviates noticeably from the (+x)-direction, this may yield a certain widening of the draping pattern perpendicular to the undisturbed flow direction. In other words, it is possible that the extension of the magnetic lobes in ($\pm$z)-direction is underestimated by a two-species simulation approach, assuming the upstream flow to consist only of a single heavy species whose flow pattern is not significantly altered. Nevertheless, comparing the magnetic field pattern in Fig. 8c with the results presented in Fig. 3 clearly indicates that this effect may only be of minor relevance, i.e. neither the qualitative structure of the draping pattern nor the peak field value in the lobes undergoes a remarkable modification when splitting up the magnetospheric upstream flow in two distinct species.

In strong analogy to the simulation presented in Sect. 4, in the polar plane, each of the three ionospheric species exhibits a narrow tail, being confined to an area with a diameter of less than $\pm 2\,R_T$ perpendicular to the flow direction. The ionospheric mass-spectrometer effect does not manifest in this cutting plane. Thus, even though in the polar plane, the flow patterns of the two upstream species are modified on different scales, the tail structure may not be adequate for a discrimination between different ionospheric populations.

The simulation results for Titan's equatorial plane are shown in Figs. 10 and 11, respectively. In analogy to the behaviour of the hypothetical $\left(N^+/H^+\right)$ ions, a slightly pronounced, but highly asymmetric cavity occurs in the Nitrogen density downstream of the obstacle. Besides, in complete correpondence to the results obtained by using a single upstream species, a cavity of reduced electric field strength is formed in the wake region. In the E^- hemisphere, this cavity is sharply confined, whereas it possesses an extension of more than $5\,R_T$ in the direction of the undisturbed convective electric field, its flank in the E^+ hemisphere forming

an angle of about 45° with the direction of the undisturbed plasma flow. A slight cavity of reduced Hydrogen density arises downstream of the obstacle (cf. Fig. 10b), its flank in the E^- hemisphere being located at the same position as the flank of the ionospheric tails and the outer boundary of the electric field cavity. As to be seen from Fig. 10e, in the E^- hemisphere, the H^+ bulk velocity is directed almost parallel to the outer flank of the electric field cavity, illustrating that this species seems to be at least partially incapable to cross the tail's boundary in the Saturn-facing hemisphere from outward to inward. The electron pressure term at the tail's flank in the E^- hemisphere has proven to be the major reason for this deflection process (Simon et al., 2006c).

In the anti-Saturn facing E^+ hemisphere, the Hydrogen ions are also deflected around the ionospheric tail region which is denoted by an enhanced density of slow ionospheric ions and, in consequence, a reduced electric field strength. As displayed in Fig. 10e, in the E^+ hemisphere, the H^+ ion velocity is directed nearly parallel to the flank of the ionospheric tail, the velocity vectors forming an angle of about 30° with the (+x)-direction. As H^+ ions are at least partially incapable of gaining access to the tail region beyond the obstacle, they are pressed against the anti-Saturn-facing flank of the ionospheric tail and are guided along this boundary layer. This gives rise to a pronounced, highly asymmetric region of enhanced Hydrogen density near the ramside of Titan.

In contrast to this, the flow pattern of the magnetospheric Nitrogen ions is practically not affected when encountering the tail's flank in the E^+ hemisphere. As to be seen in Fig. 10f, at the tail's flank in the E^+ hemisphere, the convective electric field inside the tail is directed perpendicular to the tail and pointing outward it, posing a potential barrier to any positive ion that attempts to enter the tail region from outward to inward. Even though both magnetospheric species experience the same electric field barrier, the acceleration of the heavy N^+ ions is about a factor 14 smaller than the effect on the light H^+ particles. Thus, the velocity of the N^+ ions is practically not altered, whereas a larger fraction of the H^+ ions attempting to gain access to the central tail region is decelerated, making them incapable of passing into the ionospheric tail region. In fact, the region of maximum electric field strength near the tail's anti-Saturn-facing flank in Fig. 10f can be found at the same location as the region of enhanced H^+ density. The component of the H^+ velocity tangential to the boundary layer cancels with the deceleration arising from the electric field. This yields the deflection of the H^+ flow along the flank of the electric field cavity.

However, in addition to this deflection phenomenon, the flow pattern of the H^+ ions is also affected by a second process. As displayed in Fig. 10e, at least a certain amount of the H^+ ions is able to cross the boundary of the tail in the E^+ ionosphere. Due to the reduced electric field strength in the central tail region, these H^+ ions are to a certain degree able to move antiparallel to the direction of the convective electric field and therefore to gain access to the region directly beyond the obstacle. As the magnetic field strength in the ionospheric tail region is about a factor of 1.7 smaller than in the indisturbed flow, the dynamics of the H^+ ions should be mainly governed by the electric field.

On the one hand, the velocity plot (cf. Fig. 10e) illustrates that inside the tail region itself, the H^+ ions possess a non-vanishing velocity component in (+y)-direction, i.e. antiparallel to the electric field orientation in the ionospheric tail. On the other hand, in the same region, the mean H^+ density (cf. Fig. 10b) is also increased by a factor 1.5, compared to the undisturbed upstream value of $n_{m,2}$=0.1 cm^{-3}. To sum up, those H^+ ions that have been able to cross the tail's flank in the E^+ hemisphere are capable of entering the central tail region by moving antiparallel to the electric field. Thus, these ions may be able to refill the cavity of reduced Hydrogen density that arises from the incapability of the H^+ ions to enter the ionospheric tail region by crossing the tail's flank in the E^- hemisphere. This is clearly illustrated by their mean flow velocity which is parallel to the boundary layer. Near the Saturn-facing flank of the tail, the deflection mechanism arising from the ionospheric electron pressure terms still seems to be present, but the resulting reduction of Hydrogen density is partially compensated by those H^+ ions who enter the ionospheric tail region in the E^+ hemisphere and then move antiparallel to the potenial barrier arising from the reduced electric field in the tail. This may be one reason why the cavity in the H^+ density is by far not as pronounced as in the case of Titan being exposed to a supersonic flow, where a fully developed Ion Composition Boundary is formed. In analogy to their flow pattern in the polar plane, the heavy Nitrogen ions are only minorly affected by the presence of the obstacle, i.e. their mean velocity does not exhibit a deviation from the (+x)-direction that is as remarkable as the modification of the Hydrogen flow. An explanation for this behaviour has been given above.

The high temperature of the H^+ ions must be considered a major reason for their quite complex flow pattern. Due to their low mass, they are more affected by the potential barrier at the ionospheric tail's flank in the E^+ hemisphere than the heavy N^+ ions. However, the relative velocity change $\delta v/v$ that a certain H^+ ion undergoes when attempting to cross the barrier is strongly depending on its thermal velocity. As stated above, due to their low mass, the H^+ ion can possess a thermal velocity that exceeds the mean bulk velocity of the upstream flow by more than a factor of 2. In general, the velocity of an individual ion can be obtained by adding its thermal velocity vector to the mean flow velocity:

$$\boldsymbol{v}_{s,2} = \boldsymbol{u}_{m,2} + \boldsymbol{v}_{\mathrm{th},2} \quad . \tag{44}$$

If the vectors $\boldsymbol{u}_{m,2}$ and $\boldsymbol{v}_{\mathrm{th},2}$ are parallel, the particle velocity may exceed the mean flow velocity by more than a factor of 3. Hence, the relative change $\delta v/v$ that the velocity vector of such a fast particle undergoes when attempting to cross the potential barrier is significantly smaller than the effect on a particle with a negligible thermal velocity. Thus, it is

justified to expect that especially those H^+ ions that possess a high thermal velocity parallel to $\boldsymbol{u}_{m,2}$ are able to cross the oblique tail flank from outward to inward. On the other hand, if the thermal velocity of a particle is negligible or if the two vectors in Eq. (44) are antiparallel, the particle may be forbidden to cross the potential barrier. In any case, the fraction of H^+ ions that possess a sufficiently high velocity to cross the potential barrier, and consequently the sharpness of this boundary layer, should depend on the ion temperature. In the following section, this aspect will be investigated in more detail by comparing the simulation results to the case of a H^+ component that is about a factor 5 colder than in the current scenario. This investigation will also yield new insights into the question of why the Ion Composition Boundary vanishes when Titan is located inside the Saturnian magnetosphere.

Compared to the results presented in the previous Sect. (cf. Fig. 6), the ionospheric densities displayed in Fig. 11 are around a factor 5 higher. However, the global structure of the tail is not significantly modified by splitting up the upstream flow in two distinct species. In correspondence to the results presented in the previous section, the ionospheric tail structure again exhibits the mass-spectrometer effect suggested by Luhmann (1996). Because in the central ionospheric tail the densities of slow ionospheric particles clearly exceed the magnetospheric ion density, the electric field cavity, especially its outer boundaries are sharper pronounced than in the results displayed in Fig. 5d. In the tail region, the ionospheric particles definitely make the major contribution to the convective electric field.

Compared to the results shown in Fig. 5, the magnetic pile-up region in the equatorial plane has undergone a noticeable transition. In the simulation run that used a single-species representation for the ambient magnetospheric plasma flow (cf. Sect. 4), the pile-up region in the equatorial plane possessed an extension of only about $2.5-3\,R_T$ in the direction of the convective electric field. In contrast to this, in Fig. 5c, a sharply developed enhancement of magnetic field strength is identifiable in a distance of more than $5\,R_T$ in E^+ direction, the structure of this pile-up signature coinciding with the outer flank of the ionospheric tail and the cavity in the electric field strength. The mechanism giving rise to this structure is clearly based on splitting up the magnetospheric plasma flow in two distinct components. As expressed by Eq. (43), the formation of the pile-up region is mainly based on the convection of the field lines along the magnetospheric plasma flow. Since the lighter species experiences a significant deflection, i.e. the H^+ velocity vectors a noticeably altered in the vicinity of Titan, it is evident that the magnetic field topology is also affected. The extension of the pile-up region in the E^+ hemisphere is stretched, following the motion of the H^+ ions along the oblique outer flank of the ionospheric tail.

5.2 Influence of the proton temperature

A major result of the two-species simulations presented in earlier papers has been that in the case of Titan being exposed to a supersonic flow, the ambient plasma is clearly separated from the ionospheric flow by means of an Ion Composition Boundary, whereas in the case of Titan being exposed to the slow and hot magnetospheric plasma, this boundary layer is no longer present and at most, a weak tendency to form such a boundary layer can be identified in the simulation results. One major reason that leads to the disappearence of the Ion Composition Boundary could be attributed to the changes in the ionospheric tail structure when Titan re-enters the magnetosphere: Since the density gradient near the tail's Saturn-facing flank is weaker when the obstacle is located inside the Saturnian magnetosphere, the electric force arising from the electron pressure term is too weak to forbid the magnetospheric plasma flow to gain access to the central tail region. However, the results presented in the previous section also suggest that the high thermal velocity of the ambient magnetospheric plasma is of consequence for Titan's tail structure. In fact, for the simulations presented by Simon et al. (2006c), the case of Titan's interaction with a supersonic flow has not been obtained from the inner-magnetospheric scenario by altering the alfvenic, but the sonic and magnetosonic Mach numbers of the magnetospheric flow. The temperatures of both magnetospheric ions and electrons have been reduced to generate a hypothetical scenario with a super-alfvenic, supersonic and supermagnetosonic upstream plasma.

The extent to which the high thermal velocity of the magnetospheric particles takes influence on the wake structure, especially on the sharpness of the boundaries evolving from the interaction, can be studied by analyzing the dynamics of the magnetospheric H^+ ions in the five-species simulation scenario. Due to their low mass, their flow pattern is – in contrast to the heavy N^+ and $\left(N^+/H^+\right)$ ions – clearly modified by the distorted magnetic environment of Titan. Therefore, another simulation run for the 18:00 local time scenario has been conducted, assuming the H^+ temperature to be about a factor of 5 smaller than in the run presented in the previous section.

The results of this simulation scenario are displayed in Figs. 12–14. The magnetospheric plasma parameters and the electromagnetic fields in the polar plane are to be seen in Fig. 12, whereas Figs. 13 and 14 show the situation in the equatorial plane. Both the N^+ and the H^+ ions are injected into the simulation box with a mean velocity of $\boldsymbol{u}_0 = (120\ \mathrm{km/s}, 0, 0)$. However, while the mean thermal velocity of the Nitrogen component has been set to a value of

$$v_{th} = \sqrt{\frac{3k_B T}{m}} = \sqrt{\frac{3 \cdot 2900\,\mathrm{eV}}{14\,\mathrm{amu}}} \approx 244\,\mathrm{km/s} \tag{45}$$

and therefore exceeds the mean plasma velocity by a factor of two, the mean thermal velocity of the H^+ ions is about a factor 5 smaller. Thus, the dynamics of the N^+ ions are

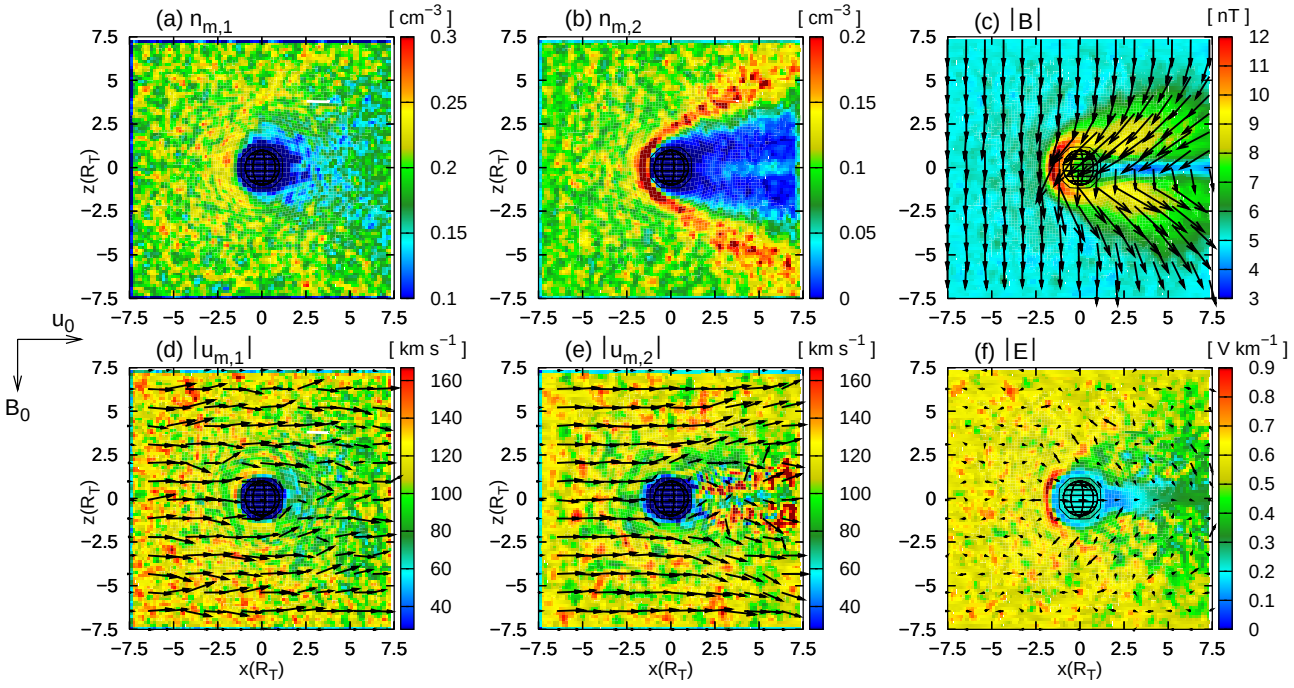

Fig. 12. Five-species simulation of Titan's plasma environment at 18:00 local time – Influence of the proton temperature. In the real Titan situation, the mean thermal velocities of magnetospheric protons and Nitrogen ions are almost equal and exceed the average velocity of the impinging magnetospheric plasma flow by a factor of 2. In order to investigate the influence of the proton temperature on the sharpness of the plasma boundaries in the vicinity of Titan, the value has been reduced by a factor of 5. For this situation, the figure displays the magnetospheric plasma parameters and the electromagnetic fields in the polar plane: **(a)** Nitrogen density, **(b)** Hydrogen density, **(c)** magnetic field, **(d)** Nitrogen velocity, **(e)** Hydrogen velocity and **(f)** electric field. As to be seen from (b), a cone-shaped cavity of nearly vanishing Hydrogen density is formed in the downstream region, its outer flanks being clearly identifiable.

governed by nondirectional thermal motion, whereas most of the H^+ ions possess a velocity vector that is almost parallel to the (+x)-direction. The influence of the reduced H^+ temperature on the plasma flow in the polar plane are displayed in Figs. 12b and e. The proton flow is now clearly deflected around the obstacle, giving rise to a cone-shaped region where the density almost vanishes. Practically no protons are present in the central tail region. As displayed in Fig. 12b, the structure of the H^+ wake exhibits a strong similarity to the cavity of reduced magnetospheric density that was formed in the case of Titan being exposed to a supersonic upstream plasma flow (see also Simon et al., 2006c). Again, the H^+ ions are pressed against the outer flanks of the central tail, but now, the density in these regions exceeds the upstream value by more than a factor of 2. Thus, the colder are the H^+ ions, the more pronounced is the mass-spectrometer effect exhibited by the magnetospheric plasma flow in the polar plane. An analogous effect occurs in the equatorial plane: The proton density is now increased along the entire tail flank in the E^+ hemisphere, the peak density in this region is more than a factor of 3 larger than the background value. However, because an analogous change manifests neither in the velocity nor in the electromagnetic fields, it is obvious that the enhancement of the H^+ density does not indicate the formation of some kind of shock-like structure, as it is developed when Titan is located outside of Saturn's magnetosphere. Besides, a definite tendency to form of an Ion Composition Boundary manifests in the proton density directly beyond Titan. A narrow region of almost vanishing H^+ density has evolved downstream of Titan, being clearly confined to the E^+ hemisphere. Since the proton temperature is the only simulation parameter that has been altered, it is obvious that the ion temperature definitely has an influence on the structure of the plasma boundaries near Titan.

The ionospheric tail region is surrounded by potential barriers: In the E^- hemisphere, the relatively sharp decrease of the ionospheric denisty gives rise to an electric field that is directed outward the tail and therefore prevents magnetospheric particles from entering the ionospheric tail region in the E^- hemisphere. On the other hand, at the tail's oblique flank in the E^+ hemisphere, it is the convective electric field inside the tail that poses a barrier to the impinging magnetospheric plasma flow.

Comparing the ionospheric densities and velocites in Fig. 14 with the situation when the magnetospheric Hydrogen component is assumed to be hot (cf. Fig. 11) clearly indicates that the ionospheric tail structure itself is not affected by altering the temperature of the magnetospheric Hydrogen

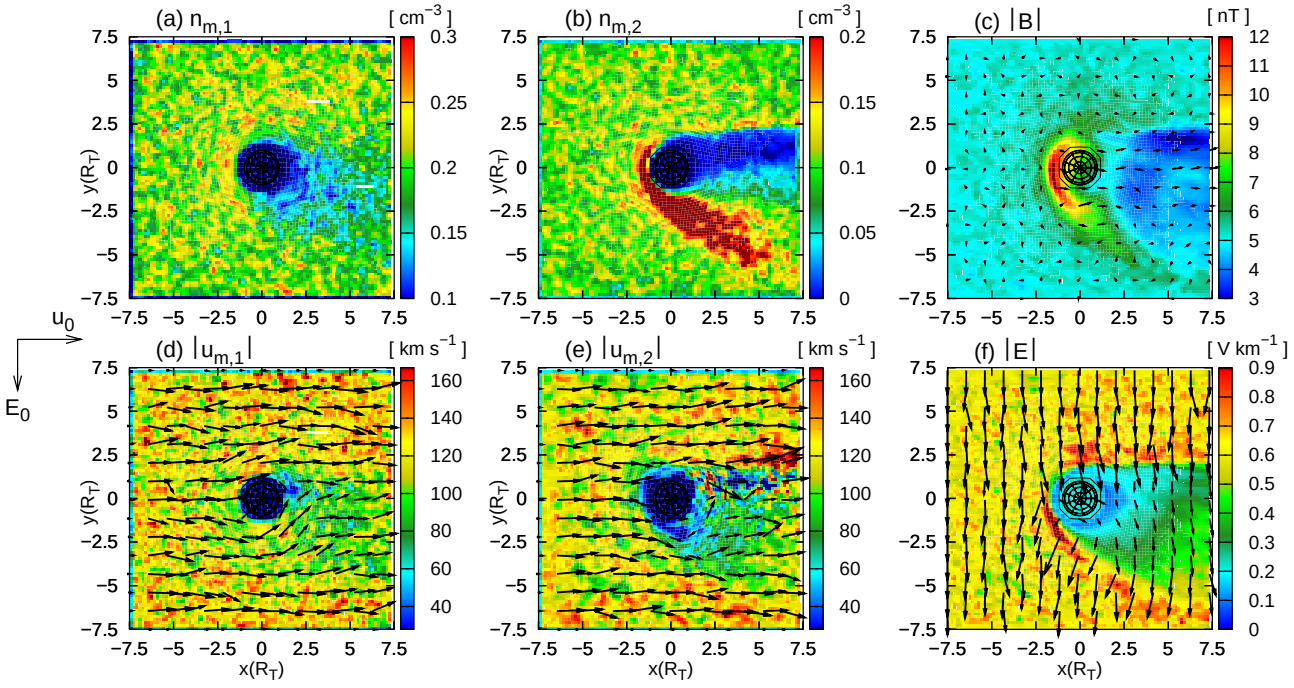

Fig. 13. Five-species simulation of Titan's plasma environment at 18:00 local time – Influence of the proton temperature. For the case of a reduced H^+ temperature, the figure displays the magnetospheric plasma parameters as well as the electromagnetic fields in the equatorial plane. Since directly beyond Titan, a pronounced cavity of reduced Hydrogen density is formed, it is obvious that the smaller is the thermal velocity of the particles, the more pronounced is the tendency to form an Ion Composition Boundary.

component. The density and velocity distribution inside the tail, but the electromagnetic fields as well, are almost identical in both simulations. Thus, both the warm and the cold protons are facing the same obstacle when encountering Titan's ionospheric tail. As will be discussed in the following, this makes the thermal velocity to be the relevant parameter for the penetration problem.

Whether a particle is able to cross these barriers is determined by two factors: first of all, the larger is the mass of an ion, the smaller is the acceleration that it experiences when encountering the potential barrier surrounding the ionospheric tail. Therefore, the effect on the Nitrogen ions, i.e. their tendency to form an Ion Composition Boundary, is not as pronounced as the deflection of the light protons around the tail region. On the other hand, the thermal velocity of the particles is of major consequence. The larger is the temperature of the protons, the more of them are able to pass the potential barrier surrounding the ionospheric tail, i.e. the Ion Composition Boundary becomes more and more penetrable. If the sum of thermal and mean velocity of an ion is sufficiently large, the relative velocity change $\delta v/v$ that it undergoes when attempting to access the ionospheric tail region is negligible, to a certain degree even for the light H^+ ions. Thus, the sensitiveness of the magnetospheric mass spectrometer can be considered a function of the temperatures of the involved ion species. In any case, if the magnetospheric hydrogen plasma is sufficiently cold, the magnetospheric mass spectrometer effect occurs in both the polar and the equatorial plane. In the polar plane, the cavity of reduced H^+ density is cone-like and symmetric, whereas in the equatorial plane, it is confined to the region directly beyond Titan, the proton density exhibiting an asymmetric structure.

Another important conclusion that can be drawn from this numerical experiment concerns the *ionospheric* mass spectrometer effect. In general, the simulation discussed in this section indicates that only if a certain plasma component is sufficiently cold, the interaction gives rise to sharply pronounced boundary layers in the corresponding density signature. The warmer is the H^+ component, the less sharp is its separation from the ionospheric plasma flow. This also means that a major condition for the formation of the *ionospheric* mass spectrometer is the low temperature of the ionospheric plasma flow. In fact, in all simulations presented here, the initial ionospheric ion temperature is set to zero, assuming that it is completely negligible compared to the magnetospheric ion temperature. A similar assumption has also proven to be adequate for the simulation of the interaction between the ionosphere of Mars and the solar wind (cf. Bößwetter et al., 2004). If the temperature of the ionospheric plasma was increased[2], the dynamics of these

[2]Of course, this would only be a hypothetical simulation scenario.

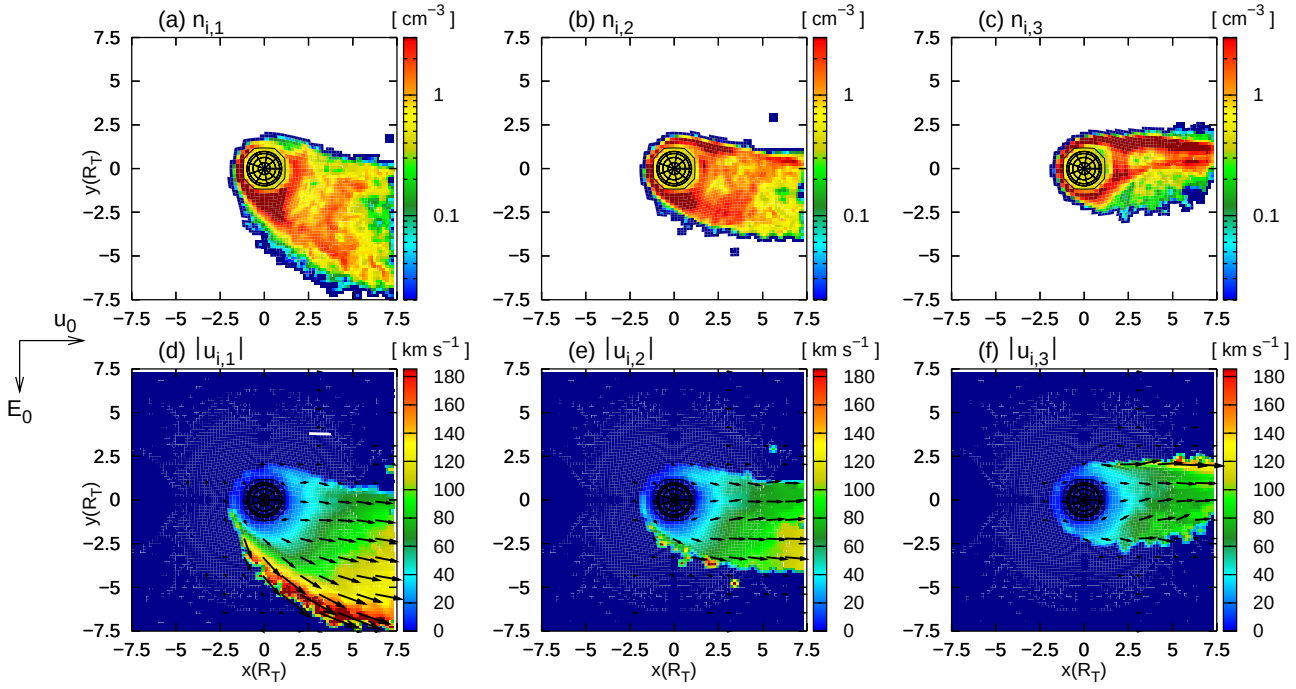

Fig. 14. Five-species simulation of Titan's plasma environment at 18:00 local time – Influence of the proton temperature. For a cut through the equatorial plane, the figure displays the ionospheric plasma densities and velocities. The characteristic features of the ionospheric tail are almost identical to the case of a warm ambient H^+ plasma flow, as displayed in Fig. 11. Therefore, the electric field barrier that the H^+ ions must pass when attempting to access the tail region is nearly the same in both cases. This is why the simulation results clearly illustrate the importance of the plasma temperature for the question of whether an Ion Composition Boundary is formed.

particles become more and more dominated by nondirectional thermal motion, which will most likely interfere with the ionospheric mass-spectrometer effect.

5.3 06:00 Saturnian local time

In the preceding sections, Titan's plasma environment at 18:00 local time has been discussed in the framework of a five-species hybrid model. It has been shown that the global features of the interaction region are well covered by a two-species approach, whereas several slight modifications of both the electromagnetic field and the ionospheric tail structures have to be attributed to the multi-species nature of the ambient magnetospheric plasma. In the following, the situation at 18:00 local time shall be compared to the case of Titan being located inside the magnetosphere at 06:00 local time, i.e. the obstacle's dayside ionosphere is assumed to be located in the wake region. As discussed by Simon et al. (2006c), the results obtained from the two-species model indicate that the situation at 06:00 local time differs only insignificantly from the case of Titan's dayside ionosphere being exposed to the upstream plasma flow.

Since in the simulation geometry, the (+x)-axis is still directed from the Sun to Titan, the undisturbed magnetospheric plasma flow is now directed antiparallel to the x-axis. The undisturbed magnetic field is assumed to be antiparallel to the z-axis, yielding a convective electric field that is directed in the anti-Saturn-facing ($y>0$) hemisphere. The simulation results for the polar plane are displayed in Figs. 15 and 16, whereas Figs. 17 and 18 illustrate the electromagnetic field signatures and plasma parameters for a cut through the equatorial plane. As to be seen from Fig. 15c, the draping pattern in the polar plane clearly resembles the magnetic signatures obtained by using a two-species hybrid model. However, in analogy to the situation at 18:00 local time, the magnetic pile-up value achieved at Titan's dayside has slightly diminished. While earlier two-species simulations show only a minor reduction of the magnetic field strength in the equatorial plane, the results obtained from the five-species model indicate that the field strength between the lobes nearly vanishes (cf. Figs. 15c and 17c). In this region, the electric field magnitude also drops to values below 0.1 Vm^{-1}. Due to the nightside of Titan being exposed to the upstream plasma flow, the density of slow ionospheric ions in the tail region exceeds the magnetospheric ion density by several orders of magnitude, yielding this strong reduction of electric field strength (cf. Fig. 17f). As in the tail region directly beyond the obstacle, neither the magnetic nor the electric field makes a significant contribution to the Lorentz force, a newly generated ionospheric particle that is entering the wake is practically not accelerated. Especially the CH_4^+ and the H_2^+ ions do

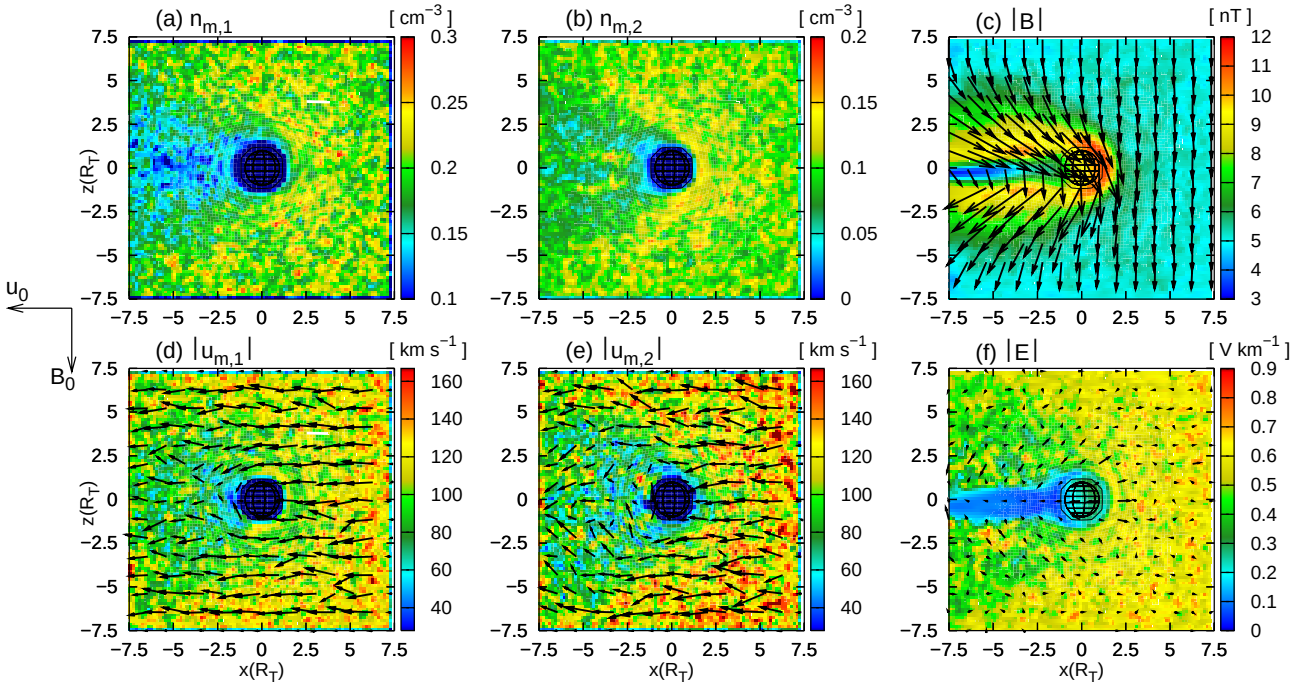

Fig. 15. Five-species hybrid simulation of Titan's plasma environment at 06:00 local time – Magnetospheric plasma parameters and electromagnetic fields in the polar plane. In correspondence to the 18:00 local time scenario, the Hydrogen ions are clearly deflected around the obstacle, whereas the magnetospheric Nitrogen flow is decelerated, but does not undergo a significant modification of its flow direction. The region of reduced magnetic field strength between the two lobes is sharper pronounced than in the results of the two-species model developed by Simon et al. (2006c): the field magnitude diminishes to values well below 3 nT.

not experience a noticeable pick-up force, since -due to their small gyroradii- their tails are almost completely located inside the cavity of reduced electromagnetic field strength. Because these particles are not transported away from the obstacle in an efficient manner, they accumulate in the vicinity of Titan, as to be seen in Fig. 18. Besides, in contrast to the 18:00 local time scenario, the region of major ion production is now located in the wake region. For this reason, the density of slow ionospheric ions in the tail clearly exceeds the densities in the 18:00 local time scenario. An accumulation of the slow ionospheric ions beyond the obstacle also occurs in the polar plane, as to be seen in Fig. 16.

The massive concentration of slow ionospheric particles, especially of Methane and Hydrogen, also yields a certain deformation of the ionospheric tail structure. In correspondence to the situation at 18:00 local time, the Nitrogen tail is clearly shifted in the direction of the convective electric field, its extension clearly exceeding the diameters of the CH_4^+ and the H_2^+ tails perpendicular to the flow direction. Again, the mass-spectrometer effect should allow to discriminate between the heavier N_2^+ ions and the two lighter species. However, as their ionospheric tails are almost completely located inside the electromagnetic field cavity beyond Titan, the pick-up of both H_2^+ and CH_4^+ ions is massively suppressed, i.e. the Lorentz forces are too weak to transport the ions away from Titan sufficiently fast and therefore to compensate for the ongoing production of new ionospheric particles. As a result of this, the flanks of both the H_2^+ and the CH_4^+ tail in the E^+ hemisphere are located nearly at the same position, making it impossible to distinguish between these two species by means of the ionospheric mass spectrometer effect. In other words, a substantial pick-up process, determined by a sufficiently high electromagnetic field strength in the tail region, must be considered a major condition for the mass spectrometer to be clearly identifiable. Besides, the tail's flank in the E^- hemisphere also undergoes a certain deformation: Compared to the two-species simulations, the ionospheric tail exhibits a widening antiparallel to the electric field. Due to their small gyroradii, this phenomenon yields an almost symmetric tail structure for the H_2^+ ions.

In the polar plane, the density signature of the magnetospheric H^+ ions qualitatively resembles the situation in the 18:00 local time scenario, showing a slight reduction of the number density beyond the obstacle. However, in the case of Titan's nightside being located in the wake region, a massive increase of H^+ density manifests near the entire flank of the ionospheric tail, as to be seen from Fig. 17b.

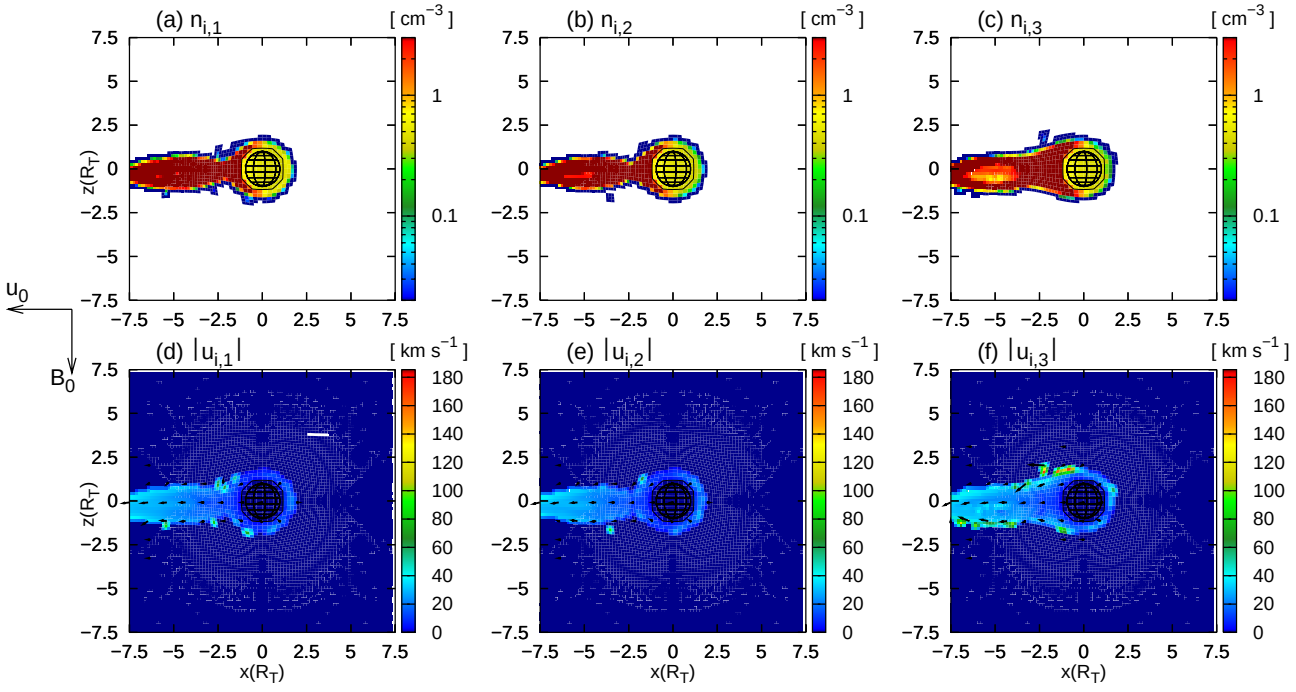

Fig. 16. Five-species hybrid simulation of Titan's plasma environment at 06:00 local time – Ionospheric densities and velocities in the polar plane. Again, the molecular Nitrogen component is denoted by the subscript 1, whereas the subscripts 2 and 3 refer to the Methane and the molecular Hydrogen component, respectively. Each of the three species forms a narrow tail directly beyond the obstacle. Because the electromagnetic field strength in the tail region almost vanishes, a newly generated ionospheric particle experiences practically no acceleration. Besides, the dayside ionosphere is now located in the wake region. Due to these two factors, the ionospheric densities in the tail are about an order of magnitude larger than in the 18:00 scenario.

6 Summary and outlook

The main objective of the work presented in this paper is the study of the interaction between the multi-species Saturnian magnetospheric plasma flow and the multi-component ionosphere of Titan. In the simulations discussed in former papers, Titan's complex ionosphere had been represented by only a single ion species (N_2^+). Therefore, in a first step, the ionosphere model has been extended to multi-species conditions by introducing Methane and molecular Hydrogen as additional species. The three selected ion species are assumed to be representative for Titan's ionosphere as the mass of N_2^+ ions is about a factor 2 larger than the mean magnetospheric ion mass, whereas the mass of CH_4^+ is comparable to the mass of the hypothetical (N^+/H^+) ions used in earlier simulations. Finally, the tail structure developed by the H_2^+ ions should illustrate the interaction of a relatively light ionospheric species with the Saturnian magnetospheric plasma.

Due to the height and the width of the cycloidal pick-up trajectories depending linearly on the particle mass, the tail's extension in the direction of the electric field is significantly different for the three species. This phenomenon may be called a *natural ion mass spectrometer* and should allow to distinguish between ions of different masses by means of spacecraft measurements. The quantitative properties of this mass spectrometer have shown to be in good agreement with both a simplified analytical model of the pick-up process and earlier test particle simulations conducted by Luhmann (1996). Compared to simulations that used a single-species ionosphere, neither the electromagnetic field topology nor the magnetospheric plasma flow in the vicinity of Titan are noticeably affected by the extension of the ionosphere model. Especially the topology of the magnetic draping pattern remains practically unaffected. In the equatorial plane, each of the three ionospheric species develops a tail that is shifted in the direction of the convective electric field.

In a second step, the multi-species ionosphere conditions have been retained and the magnetospheric upstream flow has been split up in a Nitrogen (N^+) and a Hydrogen (H^+) component. At first, the case of Titan's dayside being exposed to the upstream flow has been investigated. The dynamics of the Nitrogen ions have proven to be quite similar to the behaviour of the hypothetical (N^+/H^+) ions as the masses of these two species differ only by a factor of 1.5. The characteristics of the Nitrogen flow experience only a minor modification, i.e. a weakly pronounced cavity of reduced N^+ density arises downstream of the obstacle. The direction of the flow does not undergo significant changes. Since the mass of the H^+ ions is about a factor 14 smaller

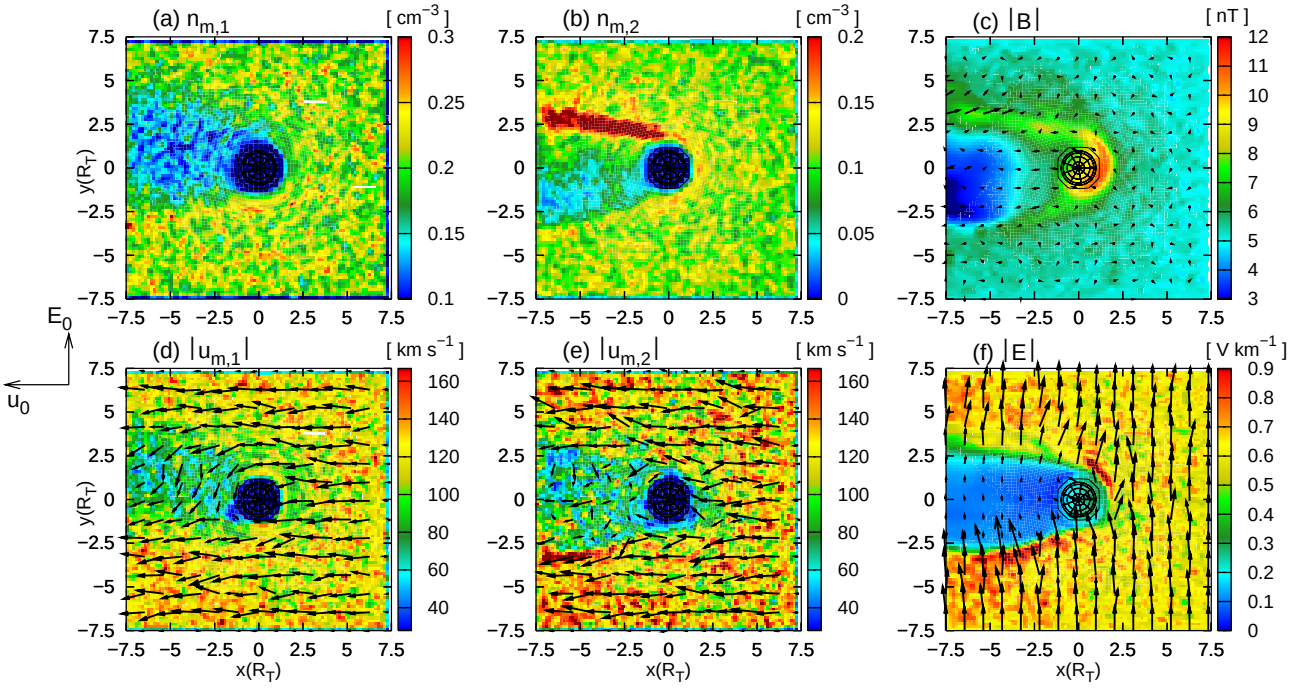

Fig. 17. Five-species hybrid simulation of Titan's plasma environment at 06:00 local time – Magnetospheric plasma parameters and electromagnetic fields in the equatorial plane. At the ionospheric tail's flank in the E^+ hemisphere, the convective electric field inside the tail poses a barrier to magnetospheric ions that try to gain access to the ionospheric tail region. Due to their smaller mass, a significant fraction of the protons is forbidden to pass this barrier. This yields a pronounced region of enhanced H^+ density along the tail's flank.

than the mass of Nitrogen, the acceleration of these particles due to the Lorentz force is more than one order of magnitude larger. Therefore, the H^+ ions are clearly deflected around the obstacle, making a certain fraction of them incapable of accessing the region directly beyond Titan. Hence, the magnetospheric plasma flow also experiences some kind of *mass spectrometer effect*. The modification of the H^+ velocities also manifests in the magnetic field topology, for the field lines are synchronously transported by the magnetospheric plasma flow. While merely a minor widening of the draping pattern manifests in the polar plane, the extension of the magnetic pile-up region in the direction of the convective electric field is increased from $3.5-4\ R_T$ to $5\ R_T$. As to be expected, the ionospheric mass-spectrometer effect is also clearly identifiable in the results of this five-species model of Titan's plasma environment. However, the separation of different ionospheric species is only present in the equatorial plane, whereas a tendency to form a magnetospheric ion mass spectrometer primarily occurs in the polar plane. The degree to which the H^+ ions are forbidden to enter the ionospheric tail region has proven to be strongly dependent on the temperature of these ions. The larger is the thermal velocity of the protons, the more of them are able to pass the potential barriers at the outer flank of the ionospheric tail and consequently, the less pronounced is the boundary separating the protons from the ionospheric plasma population.

However, it is of major importance that the simulations presented in this paper clearly illustrate the necessity of extending the simplifying model used in earlier hybrid studies of Titan's plasma environment in two distinct steps. The results obtained in the first step, i.e. including to additional ionospheric species while retaining the single-species representation of the magnetospheric flow, have shown that in the 18:00 local time scenario, upgrading the ionosphere model does neither have a remarkable effect on the electromagnetic field topology nor on the magnetospheric plasma parameters obtained from the single-species model.

The second step on the other hand, i.e. splitting up the magnetospheric plasma flow, illustrated that in the 18:00 local time case, the ionospheric tail structures are only slightly affected by altering the upstream conditions. For this reason, the major features of the ionospheric tail in the 18:00 local time scenario are almost completely covered in the framework of a single-species model for the magnetospheric plasma. The slight modification of the magnetic field topology can definitely be ascribed to the application of a more realisitc model to the upstream plasma flow. In any case, the simulation results have cleary shown that the two-species model used in chapter 4 should be capable of providing an adequate description of the magnetic field distortions in the vicinity of Titan when the obstacle's dayside is exposed to the upstream plasma flow.

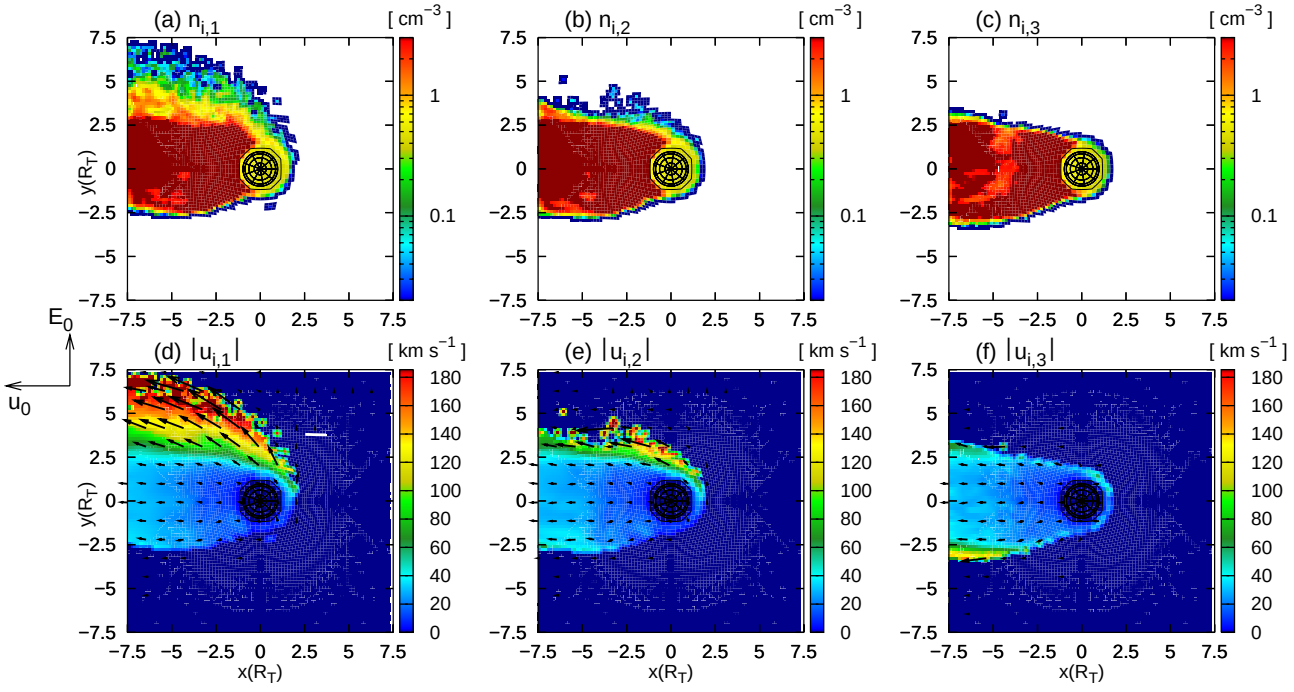

Fig. 18. Five-species hybrid simulation of Titan's plasma environment at 06:00 local time – Ionospheric densities and velocities in the equatorial plane. Since the dayside ionosphere is located in the wake region, a massive concentration of slow ionospheric particles can be found in the immediate vicinity of Titan. Especially the trajectories of newly generated CH_4^+ and H_2^+ ions are almost entirely located in the cavity of reduced electromagnetic field strength beyond the obstacle. Therefore, the transport of these particles away from Titan cannot compensate for the permanent production of new ions. This effect also yields a deformation of the tail structure. As to be seen from **(c)**, the Hydrogen tail beyond Titan exhibits an almost symmetric structure.

The second scenario that has been investigated by means of the five-species hybrid model is the case of Titan's nightside being exposed to the magnetospheric plasma at 06:00 local time. Again, the N_2^+ ions form a large and highly asymmetric tail of reduced electric field strength downstream of Titan. Due to their small gryoradii, the ionospheric tails of Methane and molecular Hydrogen are almost completely located in the region of reduced electromagnetic field strength beyond the obstacle. On the one hand because of the weak Lorentz forces acting on these ions, on the other hand because the region of major ion production is located in the wake, the ionospheric densities in the tail are about an order of magntitude larger than in the 18:00 local time scenario. The accumulation of ionospheric particles in the vicinity of Titan also yields a certain deformation of the tail structures, i.e. a discrimination between CH_4^+ and H_2^+ by means of the ionospheric mass spectrometer is no longer possible. Besides, compared to the two-species simulation presented by Simon et al. (2006c) the tail extension in the E^- hemisphere has clearly increased. In combination with their small gyroradii, this effect yields an almost symmetric tail structure for Methane and Hydrogen ions.

A major aspect of our future work will be to adress the following problems: Reproduction of the global magnetic field topology detected during specific Cassini flybys will be one objective of future simulations. Especially, it will be interesting to know to what degree the data obtained by the Cassini magnetometer are reproducible in the framework of the multi-species hybrid model.

Moreover, it will be interesting to know whether evidence for the ionospheric mass spectrometer effect can be identified in data from the Cassini plasma spectrometer, as it has been suggested by Luhmann (1996) for the Voyager 1 scenario. The crucial question will be whether the ambient magnetospheric flow is sufficiently homogeneous to allow the formation of the mass spectrometer. Since according to our simulations, the formation of a spatially dispersive ionospheric tail is favored when Titan's dayside is facing the magnetospheric plasma flow, a pass through Titan's wake between 12:00 and 00:00 local time will be of interest.

Besides, during neither of the first Cassini flybys, the magnetic field was observed to be exactly perpendicular to Titan's orbital plane (Neubauer et al., 2006). The degree to which the global structure of Titan's plasma environment is affected by the orientation of the background magnetic field with respect to the impinging flow direction will be discussed in a companion paper by the same authors, referring to the T9 flyby of Cassini.

Acknowledgements. This work has been supported by the Deutsche Forschungsgemeinschaft through the grants MO 539/13-1 and MO 539/15-1.

Topical Editor I. A. Daglis thanks P. Israelevich and C. Mazelle for their help in evaluating this paper.

References

Backes, H.: Titan's Interaction with the Saturnian Magnetospheric Plasma, Ph.D. thesis, Universität zu Köln, 2005.

Backes, H., Neubauer, F. M., Dougherty, M. K., Achilleos, N., André, N., Arridge, C. S., Bertucci, C., Jones, G. H., Khurana, K. K., Russell, C. T., and Wennmacher, A.: Titan's Magnetic Field Signature During the First Cassini Encounter, Science, 308, 992–995, 2005.

Bagdonat, T.: Hybrid Simulation of Weak Comets, Ph.D. thesis, Technische Universität Braunschweig, 2004.

Bagdonat, T. and Motschmann, U.: 3D hybrid simulation of solar wind interaction with comets, in Space Plasma Simulation – Proceedings of the Sixth International School/ Symposium ISSS-6, edited by: Büchner, J., Dum, C., and Scholer, M., 80–83, 2001.

Bagdonat, T. and Motschmann, U.: 3D Hybrid Simulation Code Using Curvilinear Coordinates, J. of Computational Physics, 183, 470–485, 2002a.

Bagdonat, T. and Motschmann, U.: From a weak to a strong comet – 3D global hybrid simulation studies, Earth, Moon and Planets, 90, 305–321, 2002b.

Bößwetter, A., Bagdonat, T., Motschmann, U., and Sauer, K.: Plasma boundaries at Mars: a 3-D simulation study, Ann. Geophys., 22, 4363–4379, 2004, http://www.ann-geophys.net/22/4363/2004/.

Brecht, S., Luhmann, J. G., and Larson, D. J.: Simulation of the Saturnian magnetospheric interaction with Titan, J. Geophys. Res., 105, 13 119–13 130, 2000.

Cravens, T. E., Lindgren, C. J., and Ledvina, S. A.: A two-dimensional multifluid MHD model of Titan's plasma environment, Planet. Space Sci., 46, 1193–1205, 1998.

Cravens, T. E., Robertson, I. P., Waite, J. H., Yelle, R. V., Kasprzak, W. T., Keller, C. N., Ledvina, S. A., Niemann, H. B., Luhmann, J. G., McNutt, R. L., Ip, W.-H., De La Haye, V., Mueller-Wodarg, I., Wahlund, J.-E., Anicich, V. G., and Vuitton, V.: Composition of Titan's ionosphere, Geophys. Res. Lett., 33, L07 105, 1–4 (doi:10.1029/2005GL025 575), 2006.

Kabin, K., Gombosi, T. I., DeZeeuw, D. L., Powell, K. G., and Israelevich, P. L.: Interaction of the Saturnian magnetosphere with Titan: Results of a three-dimensional MHD simulation, J. Geophys. Res., 104, 2451–2458, 1999.

Kabin, K., Israelevich, P. L., Ershkovich, A. I., Neubauer, F. M., Gombosi, T. I., DeZeeuw, D. L., and Powell, K. G.: Titan's magnetic wake: Atmospheric or magnetospheric interaction, J. Geophys. Res., 105, 10 761–10 770, 2000.

Kallio, E., Sillanpää, I., and Janhunen, P.: Titan in subsonic and supersonic flow, Geophys. Res. Lett., 31, L15 703/1–L15 703/4, 2004.

Keller, C., Cravens, T., and Gan, L.: One-dimensional multispecies magnetohydrodynamic model of the ramside ionosphere of Titan, J. Geophys. Res., 99, 6511–6525, 1994.

Keller, C., Anicich, V., and Cravens, T. E.: Model of Titans ionosphere with detailed hydrocarbon chemistry, Planet. Space Sci., 46, 1157–1174, 1998.

Keller, C. N. and Cravens, T. E.: One-dimensional, multispecies hydrodynamic models of the wakeside ionosphere of Titan, J. Geophys. Res., 99, 6527–6536, 1994.

Keller, C. N., Cravens, T. E., and Gan, L.: A Model of the Ionosphere of Titan, J. Geophys. Res., 97, 12 117–12 135, 1992.

Kivelson, M. G. and Russell, C. T.: The Interaction of Flowing Plasmas With Planetary Ionospheres: A Titan-Venus Comparison, J. Geophys. Res., 88, 49–57, 1983.

Kopp, A. and Ip, W.-H.: Asymmetric mass loading effect at Titans ionosphere, J. Geophys. Res., 106, 8323–8332, 2001.

Ledvina, S. A. and Cravens, T. E.: A three-dimensional MHD model of plasma flow around Titan, Planet. Space Sci., 46, 1175–1191, 1998.

Ledvina, S. A., Luhmann, J. G., Brecht, S. H., and Cravens, T. E.: Titan's induced magnetosphere, Adv. Space Res., 33, 2092–2102, 2004.

Luhmann, J. G.: Titan's ion exosphere wake: A natural ion mass spectrometer?, J. Geophys. Res., 101(E2), 29 387–29 393, 1996.

Luhmann, J. G., Russell, C. T., Schwingenschuh, K., and Yeroshenko, Y.: A comparison of induced magnetotails of planetary bodies: Venus, Mars and Titan, J. Geophys. Res., 96, 11 199–11 208, 1991.

Ma, Y., Nagy, A., Cravens, T., Sokolov, I., Clark, J., and Hansen, K.: 3-D global MHD prediction for the first close flyby of Titan by Cassini, Geophys. Res. Lett., 31, L22 803(1–4), 2004.

Ma, Y., Nagy, A. F., Cravens, T. E., Sokolov, I. V., Hansen, K. C., Wahlund, J.-E., Crary, F. J., Coates, A. J., and Dougherty, M. K.: Comparisons between MHD model calculations and observations of Cassini flybys of Titan, J. Geophys. Res., 111, A05 207, doi:10.1029/2005JA011481, 2006.

Modolo, R.: Modelisation de l' interaction du vent solaire, ou du plasma Kronien, avec les environnements neutres de Mars et de Titan, Ph.D. thesis, L' universite de Versailles Saint-Quentin-en-Yvelines, 2004.

Nagy, A., Liu, Y., Hansen, K., Kabin, K., Gombosi, T., Combi, M., and DeZeeuw, D.: The interaction between the magnetosphere of Saturn and Titans ionosphere, J. Geophys. Res., 106, 6151–6160, 2001.

Nagy, A. F. and Cravens, T. E.: Titans ionsophere: A review, Planet. Space Sci., 46, 1149–1155, 1998.

Ness, N., Acuna, M., Behannon, K., and Neubauer, F.: The induced magnetosphere of Titan, J. Geophys. Res., 87, 1369–1381, 1982.

Neubauer, F. M., Gurnett, D. A., Scudder, J. D., and Hartle, R. E.: Titan's magnetospheric interaction, in Saturn, edited by T. Gehrels and M. S. Matthews, University of Arizona Press, Tucson, Arizona, 760–787, 1984.

Neubauer, F. M., Backes, H., Dougherty, M. K., Wennmacher, A., Russell, C. T., Coates, A., Young, D., Achilleos, N., Andre, N., Arridge, C. S., Bertucci, C., Jones, G. H., Khurana, K. K., Knetter, T., Law, A., Lewis, G. R., and Saur, J.: Titan's near magnetotail from magnetic field and plasma observations and modelling: Cassini flybys TA, TB and T3, J. Geophys. Res., 111, A10 220 (1–15), doi:10.1029/2006JA011676, 2006.

Roboz, A. and Nagy, A. F.: The energetics of Titan's ionosphere, J. Geophys. Res., 99, 2087–2093, 1994.

Schardt, A. W., Behannon, K. W., Lepping, R. P., Carbary, J. F., Eviatar, A., and Siscoe, G. L.: The outer magnetosphere, in: Saturn, edited by: Gehrels, T. and Matthews, M. S., University of

Arizona Press, Tucson, 416–459, 1984.
Sillanpää, I., Kallio, E., Janhunen, P., Schmidt, W., Mursula, K., Vilppola, J., and Tanskanen, P.: Hybrid simulation study of ion escape at Titan for different orbital positions, Adv. Space Res., in press, 2006.
Simon, S., Bagdonat, T., Motschmann, U., and Glassmeier, K.-H.: Plasma environment of magnetized asteroids: a 3-D hybrid simulation study, Ann. Geophys., 24, 407–414, 2006a.
Simon, S., Bösswetter, A., Bagdonat, T., and Motschmann, U.: Physics of the Ion Composition Boundary: A comparative 3-D hybrid simulation study of Mars and Titan, Ann. Geophys., 25, 99–115, 2006b.
Simon, S., Bösswetter, A., Bagdonat, T., Motschmann, U., and Glassmeier, K.-H.: Plasma environment of Titan: a 3-d hybrid simulation study, Ann. Geophys., 24, 1113–1135, 2006c.
Verigin, M. I., Gringauz, K. I., and Ness, N. F.: Comparison of induced magnetospheres at Venus and Titan, J. Geophys. Res., 89, 5461–5470, 1984.
Wahlund, J.-E., Boström, R., Gustafsson, G., Gurnett, D. A., Kurth, W. S., Pedersen, A., Averkamp, T. F., Hospodarsky, G. B., Persoon, A. M., Canu, P., Neubauer, F. M., Dougherty, M. K., Eriksson, A. I., Morooka, M. W., Gill, R., André, M., Eliasson, L., and Mueller-Wodarg, I.: Cassini Measurements of Cold Plasma in the Ionosphere of Titan, Science, 308, 986–989, 2005.
Wolf, D. A. and Neubauer, F. M.: Titan's Highly Variable Plasma Environment, J. Geophys. Res., 87, 881–885, 1982.